

**ANALYSIS OF ONE WAY VALVE MECHANISM FOR
WINGS OF A FLAPPING DRONE**

DENG XINCHEN

**FACULTY OF ENGINEERING
UNIVERSITY OF MALAYA
KUALA LUMPUR**

2020

**ANALYSIS OF ONE WAY VALVE MECHANISM FOR
WINGS OF A FLAPPING DRONE**

DENG XINCHEN

**RESEARCH PROJECT SUBMITTED IN FULFILMENT
OF THE REQUIREMENTS FOR THE DEGREE OF
MASTER OF MECHANICAL ENGINEERING**

**FACULTY OF ENGINEERING
UNIVERSITY OF MALAYA
KUALA LUMPUR**

2020

UNIVERSITY OF MALAYA
ORIGINAL LITERARY WORK DECLARATION

Name of Candidate: Deng Xinchun

Matric No: KQK180031

Name of Degree: Master of Mechanical Engineering

Title of Research Project: Analysis of one way valve mechanism for wings of a flapping drone

Field of Study:

Aerospace, Mechanical and Computer Fluid Dynamic Analysis

I do solemnly and sincerely declare that:

- (1) I am the sole author/writer of this Work;
- (2) This Work is original;
- (3) Any use of any work in which copyright exists was done by way of fair dealing and for permitted purposes and any excerpt or extract from, or reference to or reproduction of any copyright work has been disclosed expressly and sufficiently and the title of the Work and its authorship have been acknowledged in this Work;
- (4) I do not have any actual knowledge nor do I ought reasonably to know that the making of this work constitutes an infringement of any copyright work;
- (5) I hereby assign all and every rights in the copyright to this Work to the University of Malaya ("UM"), who henceforth shall be owner of the copyright in this Work and that any reproduction or use in any form or by any means whatsoever is prohibited without the written consent of UM having been first had and obtained;
- (6) I am fully aware that if in the course of making this Work I have infringed any copyright whether intentionally or otherwise, I may be subject to legal action or any other action as may be determined by UM.

Candidate's Signature

Date:

Subscribed and solemnly declared before,

Witness's Signature

Date:

Name:

Designation:

ANALYSIS OF ONE WAY VALVE MECHANISM FOR WINGS OF A FLAPPING DRONE

ABSTRACT

The flapping drone is one type of MAVs which is defined as a miniature unmanned aerial vehicle that is inspired by flying birds and insects. Flapping wings can make a perfect combination of thrust and lift by flapping up and down with full usage of unsteady air. The flapping drone has the advantages of high maneuverability and a special lift generation mechanism. Compared with rotary-wing or fixed-wing MAV, it is smaller, lighter, and has higher flight performance. It can quickly change the flight direction and flight speed by control the flapping frequency and it is the only flight mode that does not cause a stall. Therefore, flapping drones have great use value and prospects in the military and civilian fields. However, flapping drones have some disadvantages. Its wings only have one degree of freedom which makes it can only flap up and down so that the drag force created by flapping is always equal. This phenomenon affects the flight ability of drones.

The primary and secondary feathers of birds can cover and separate from each other. The feathers cover each other to increase the lift during the upstroke of wings and open to create a gap to reduce the drag during the downstroke. According to this mechanism, this research studied the one way valve mechanism to investigate the effects of one way valve on flight performance of flapping drones.

There are two parts of this research. The first part used ANSYS software to create several models of one way valve mechanism including single valve and two valves, different air inlets and four types of valve opening angles. Then CFD simulation was used to test the performance of these models. According to the comparison of the results, the conclusion is that the one way valves perform the most effective when the angle of the opening in the range of 30° and 45°.

The second part used actual experiment to test the one way valve wings. There are four types of wings were designed, produced and tested the flight performance in this research. Four wings were also measured the velocity generated by wings on a test platform. The result of the actual experiment got similar conclusions with CFD simulation which is the one way valve with reasonable layouts on flapping wings can improve the flight capability of flapping drones.

Keywords: Flapping wing, CFD, Lift, Drag, One way valve

University of Malaya

ANALYSIS OF ONE WAY VALVE MECHANISM FOR WINGS OF A FLAPPING DRONE

ABSTRAK

Dron kepakan adalah salah satu jenis MAV yang ditakrifkan sebagai kenderaan udara tanpa pemandu miniatur yang diilhamkan oleh burung dan serangga terbang. Sayap kepakan dapat menjadikan kombinasi dorong dan angkat sempurna dengan kepakan ke atas dan ke bawah dengan penggunaan udara yang tidak stabil sepenuhnya. Dron kepakan mempunyai kelebihan kemampuan manuver tinggi dan mekanisme penjanaan angkat khas. Berbanding dengan MAV sayap putar atau sayap tetap, ia lebih kecil, lebih ringan, dan mempunyai prestasi penerbangan yang lebih tinggi. Ia dengan cepat dapat mengubah arah penerbangan dan kecepatan penerbangan dengan mengawal frekuensi mengepak dan itu adalah satu-satunya mod penerbangan yang tidak menyebabkan berhenti. Oleh itu, dron terbang mempunyai nilai dan prospek penggunaan yang besar dalam bidang ketenteraan dan orang awam. Walau bagaimanapun, dron kepakan mempunyai beberapa kelemahan. Sayapnya hanya memiliki satu darjah kebebasan yang membuatnya hanya dapat kepakan ke atas dan ke bawah sehingga daya seret yang dibuat dengan kepakan selalu sama. Fenomena ini mempengaruhi kemampuan penerbangan dron.

Bulu burung primer dan sekunder dapat menutup dan memisahkan antara satu sama lain. Bulu berdekatan antara satu sama lain untuk meningkatkan daya angkat semasa kenaikan sayap dan terbuka untuk membuat jurang untuk mengurangkan seretan semasa hentakan bawah. Mengikut mekanisme ini, penyelidikan ini mengkaji mekanisme injap sehalu untuk mengkaji kesan injap sehalu terhadap prestasi penerbangan drone flapping.

Terdapat dua bahagian dalam penyelidikan ini. Bahagian pertama menggunakan perisian ANSYS untuk membuat beberapa model mekanisme injap sehalu termasuk injap tunggal dan dua injap, saluran masuk udara yang berbeza dan empat jenis sudut bukaan injap. Kemudian simulasi CFD digunakan untuk menguji prestasi model-model ini.

Berdasarkan perbandingan hasilnya, dapat disimpulkan bahawa injap sehalah berfungsi paling efektif apabila sudut bukaan berada dalam lingkungan 30° dan 45° .

Bahagian kedua menggunakan eksperimen sebenar untuk menguji sayap injap sehalah. Terdapat empat jenis sayap yang dirancang, dihasilkan dan diuji prestasi penerbangan dalam penyelidikan ini. Empat sayap juga diukur halaju yang dihasilkan oleh sayap pada platform ujian. Hasil eksperimen sebenar mendapat kesimpulan yang serupa dengan simulasi CFD yang merupakan injap sehalah dengan susun atur yang munasabah pada sayap kepakan dapat meningkatkan kemampuan penerbangan dron kepakan.

Kata kunci: Sayap kepakan, CFD, Angkat, Seret, Injap sehalah

University of Malaysia

ACKNOWLEDGEMENTS

First of all, I want to thank Dr. Poo Balan Ganesan, under his guidance I can complete this research study. And because of him, I can get an opportunity to work as his research assistant for six months and have the experience to do the research in the aerospace laboratory. Next thing I want to send my gratitude to my fellow teammates under this flapping drone project especially Ali who is the team leader who always checks on my work progress to ensure the success of it. Special thanks again to my supervisor Dr. Poo Balan for continuously monitor my research result and have meetings with us on the progress each week during the timeline of completing the project. Furthermore, I would like to thank my teammate Chai Yuan who is doing the same project but the different part with me. With the cooperation of each other, we able to accomplish the project smoothly and achieve an efficient result.

TABLE OF CONTENTS

Analysis of one way valve mechanism for wings of a flapping drone Abstract.....	iii
Analysis of one way valve mechanism for wings of a flapping drone Abstrak.....	v
Acknowledgements	7
Table of Contents	8
List of Figures	11
List of Tables.....	14
List of Symbols and Abbreviations.....	16
List of Appendices	18
CHAPTER 1: INTRODUCTION.....	19
1.1 Introduction.....	19
1.2 Problem statement	19
1.3 Objectives	20
1.4 Research Scope.....	20
1.5 Report outline	20
CHAPTER 2: INTRODUCTION.....	22
2.1 Background.....	22
2.2 Flapping mode	24
2.3 Overall design of flapping drone	26
2.4 Flapping Wings.....	28
2.5 FWMAVs prototype	31
2.6 Research gap.....	33
CHAPTER 3: RESEARCH METHODOLOGY	35

3.1	Computer Fluent Dynamics	35
3.1.1	Geometry	36
3.1.2	Meshing	37
3.1.3	Governing equation – continuity and momentum.....	40
3.1.4	Properties/Numerical method.....	42
3.1.5	Simulation cases	46
3.1.6	Mesh dependency investigation and validation.....	46
3.2	Experimental model and measurement method.....	49
3.2.1	Materials	49
3.2.2	Shape	50
3.2.3	Model.....	51
3.2.4	Measurements and instruments	53
CHAPTER 4: RESULTS & DISCUSSION		55
4.1	CFD results	55
4.1.1	Mass flow rate	55
4.1.1.1	Single valve with laminar model.....	57
4.1.1.2	Single valve with Transition SST model.....	61
4.1.1.3	Double valves with laminar model.....	66
4.1.1.4	Double valves with Transition SST model	70
4.1.2	Velocity streamline.....	74
4.1.3	Pressure	76
4.1.4	Lift and drag	79
4.2	Experimental.....	82
4.2.1	Actual model	82
4.2.2	Testing flight performance	82
4.2.3	Velocity profile.....	84

CHAPTER 5: CONCLUSIONS.....	89
5.1 Future work.....	89
REFERENCES	91
Appendix A.....	98
Appendix B	100
Appendix C	102

University of Malaya

LIST OF FIGURES

Figure 1.1 Flapping wing mechanism.....	19
Figure 2.1 Microbat from California Institute of Technology.	26
Figure 2.2 Entomopters from Georgia Institute of Technology.....	27
Figure 2.3 Hummingbird FWMAVs wing structure.....	27
Figure 2.4 FlowerFly from National University of Singapore.....	28
Figure 2.5 Some wing types during NAV project implementation	29
Figure 2.6 The intact and perforated wing test model from Long Chen (2015).....	30
Figure 2.7 DelFly Explorer (1) Brushless motors (2) An autopilot with a complete IMU (3) Ailerons (4) The onboard stereo vision system.....	33
Figure 3.1 Flow chart of numerical simulation of wings motion.....	35
Figure 3.2 Dimensions of wind tunnel for one way valve mechanism.....	36
Figure 3.3 Dimensions of two valves wind tunnel.....	37
Figure 3.4 One valve at 45 degrees with 2 inlets	38
Figure 3.5 One valve at 45 degrees with 3 inlets	39
Figure 3.6 Two valves at 45 degrees with 2 inlets.....	39
Figure 3.7 Two valves at 45 degrees with 3 inlets.....	40
Figure 3.8 Line chart of drag force under different mesh elements.....	47
Figure 3.9 Line chart of drag force under different inflation maximum layers	49
Figure 3.10 The structure and a plan form view of the wing.....	51
Figure 3.12 Three types of experimental model	52
Figure 3.11 Tools for making wings.....	52
Figure 3.13 Hot wire anemometer	53
Figure 3.14 Measurement of velocity generated by wings	54
Figure 3.15 The design points for measuring the velocity profile.....	54

Figure 4.1 Single valve with 2 inlet (type 1).....	55
Figure 4.2 Single valve with 3 inlets (type 2).....	55
Figure 4.3 Double valves with 2 inlets (type 3).....	56
Figure 4.4 Double valves with 3 inlets (type 4).....	56
Figure 4.5 Velocity streamline of one valve mechanism at 4 types of degree with two inlets.....	74
Figure 4.6 Velocity streamline of one valve mechanism at 4 types of degree with three inlets.....	75
Figure 4.7 Velocity streamline of two valves mechanism at 4 types of degree with two inlets.....	75
Figure 4.8 Velocity streamline of two valves mechanism at 4 types of degree with three inlets.....	76
Figure 4.9 Pressure contour of one valve mechanism at 4 types of degree with two inlets.....	77
Figure 4.10 Pressure contour of one valve mechanism at 4 types of degree with three inlets.....	77
Figure 4.11 Pressure contour of two valves mechanism at 4 types of degree with two inlets.....	78
Figure 4.12 Pressure contour of two valves mechanism at 4 types of degree with three inlets.....	78
Figure 4.13 Actual flight of testing I	83
Figure 4.14 Actual flight of testing II	84
Figure 4.15 Velocity Z at Z=100mm. Type 2 wing (Left) non-valve wing (Right) and type 3 wing (Below).....	85
Figure 4.16 Velocity Y at Z=100mm. Type 2 wing (Left) non-valve wing (Right) and type 3 wing (Below).....	85
Figure 4.17 Velocity Y at Z=0. Type 2 wing (Left) non-valve wing (Right) and type 3 wing (Below).....	86
Figure 4.18 Velocity Z at Z=-100mm. Type 2 wing (Left) non-valve wing (Right) and type 3 wing (Below).....	86

Figure 4.19 Velocity Y at Z=-100mm. Type 2 wing (Left) non-valve wing (Right) and type 3 wing (Below).....87

University of Malaya

LIST OF TABLES

Table 2.1 Representative FWMAVs	31
Table 3.1 Mesh dependency test on element size	47
Table 3.2 Mesh dependency test on inflation layers	48
Table 3.3 The parameters of several typical plastic film materials.....	50
Table 4.1 Mass flow rate of single valve at 45 degrees with 2 inlets	57
Table 4.2 Mass flow rate of single valve at 30 degrees with 2 inlets	58
Table 4.3 Mass flow rate of single valve at 15 degrees with 2 inlets	58
Table 4.4 Mass flow rate of single valve at 3 degrees with 2 inlets	59
Table 4.5 Mass flow rate of single valve at 45 degrees with 3 inlets	59
Table 4.6 Mass flow rate of single valve at 30 degrees with 3 inlets	60
Table 4.7 Mass flow rate of single valve at 15 degrees with 3 inlets	60
Table 4.8 Mass flow rate of single valve at 3 degrees with 3 inlets	61
Table 4.9 Mass flow rate of single valve at 45 degrees with 2 inlets	62
Table 4.10 Mass flow rate of single valve at 30 degrees with 2 inlets	62
Table 4.11 Mass flow rate of single valve at 15 degrees with 2 inlets	63
Table 4.12 Mass flow rate of single valve at 3 degrees with 2 inlets	63
Table 4.13 Mass flow rate of single valve at 45 degrees with 3 inlets	64
Table 4.14 Mass flow rate of single valve at 30 degrees with 3 inlets	64
Table 4.15 Mass flow rate of single valve at 15 degrees with 3 inlets	65
Table 4.16 Mass flow rate of single valve at 3 degrees with 3 inlets	65
Table 4.17 Mass flow rate of double valves at 45 degrees with 2 inlets	66
Table 4.18 Mass flow rate of double valves at 30 degrees with 2 inlets	66
Table 4.19 Mass flow rate of double valves at 15 degrees with 2 inlets	67

Table 4.20 Mass flow rate of double valves at 3 degrees with 2 inlets.....	67
Table 4.21 Mass flow rate of double valves at 45 degrees with 3 inlets	68
Table 4.22 Mass flow rate of double valves at 30 degrees with 3 inlets	68
Table 4.23 Mass flow rate of double valves at 15 degrees with 3 inlets	69
Table 4.24 Mass flow rate of double valves at 3 degrees with 2 inlets.....	69
Table 4.25 Mass flow rate of double valves at 45 degrees with 2 inlets	70
Table 4.26 Mass flow rate of double valves at 30 degrees with 2 inlets	70
Table 4.27 Mass flow rate of double valves at 15 degrees with 2 inlets	71
Table 4.28 Mass flow rate of double valves at 3 degrees with 2 inlets.....	71
Table 4.29 Mass flow rate of double valves at 45 degrees with 3 inlets	72
Table 4.30 Mass flow rate of double valves at 30 degrees with 3 inlets	72
Table 4.31 Mass flow rate of double valves at 15 degrees with 3 inlets	73
Table 4.32 Mass flow rate of double valves at 45 degrees with 3 inlets	73
Table 4.33 Drag force and CD for different type valves at 45 degrees valve angle	79
Table 4.34 Drag force and CD for different type valves at 30 degrees valve angle	79
Table 4.35 Drag force and CD for different type valves at 15 degrees valve angle	80
Table 4.36 Drag force and CD for different type valves at 3 degrees valve angle	80
Table 4.37 Lift force and CF for different type valves at 45 degrees valve angle.....	80
Table 4.38 Lift force and CF for different type valves at 30 degrees valve angle.....	81
Table 4.39 Lift force and CF for different type valves at 15 degrees valve angle.....	81
Table 4.40 Lift force and CF for different type valves at 3 degrees valve angle.....	81
Table 4.41 Testing results of four types of wings.....	83
Table 4.42 Velocity description at three plane for three types of wings.....	88

LIST OF SYMBOLS AND ABBREVIATIONS

ρ	:	Fluid density
t	:	Time
u	:	The component of the fluid velocity in the x axis direction
v	:	The component of the fluid velocity in the y axis direction
w	:	The component of the fluid velocity in the z axis direction
p	:	Pressure of the fluid unit
$\tau_{xx}, \tau_{xy}, \tau_{xz}$:	Component of the viscous force on the fluid element unit surface
F_x	:	Volume force of the fluid unit in the x directions
F_y	:	Volume force of the fluid unit in the y directions
F_z	:	Volume force of the fluid unit in the z directions
h	:	Enthalpy
k_{eff}	:	Effective thermal conductivity
J_j	:	Diffusion flux
S_h	:	Volume heat source term including chemical reaction heat
Re_f	:	Reynolds number during flight
\emptyset	:	Flapping amplitude of wings
f	:	Flapping frequency
l	:	Span length
ν_1	:	Kinematic viscosity of fluid
AR	:	Aspect ratio
Re_v	:	Reynolds number of valve
ν	:	Dynamic viscosity of fluid
V	:	Flow speed of fluid
C_d	:	Coefficient of drag

C_l	:	Coefficient of lift
L	:	Lift force
D	:	Drag force
m	:	Mass flow rate
A	:	Cross section area

University of Malaya

LIST OF APPENDICES

Appendix A: Sketch drawing for wing component	94
Appendix B: Sketch drawing for three types of wing	96
Appendix C: Velocity recorded data	98

University of Malaya

CHAPTER 1: INTRODUCTION

1.1 Introduction

Micro air vehicles (MAVs) were first proposed in the 1990s (J. M. McMichael, 1997). It is defined as a miniature unmanned aerial vehicle. The smallest size of MAVs is only 5 cm at present. Flapping drone is one type of MAVs which has the longest development history. After the 21st century, research on MAV has increased rapidly. Researchers keep trying to improve the flapping drone to make it have better flight ability and longer battery life. This research studies the wings of a flapping drone.

1.2 Problem statement

The principle of a flapping drone is to generate enough lift to provide flight through the flapping of wings. However, the wings only have one degree of freedom. It can only flap up and down so that the drag force created by flapping is always equal. And it has a great impact on the flight. Figure 1.1 shows the flapping wing mechanism. This research is to explore a way to reduce upward resistance and improve flying ability by 30%.

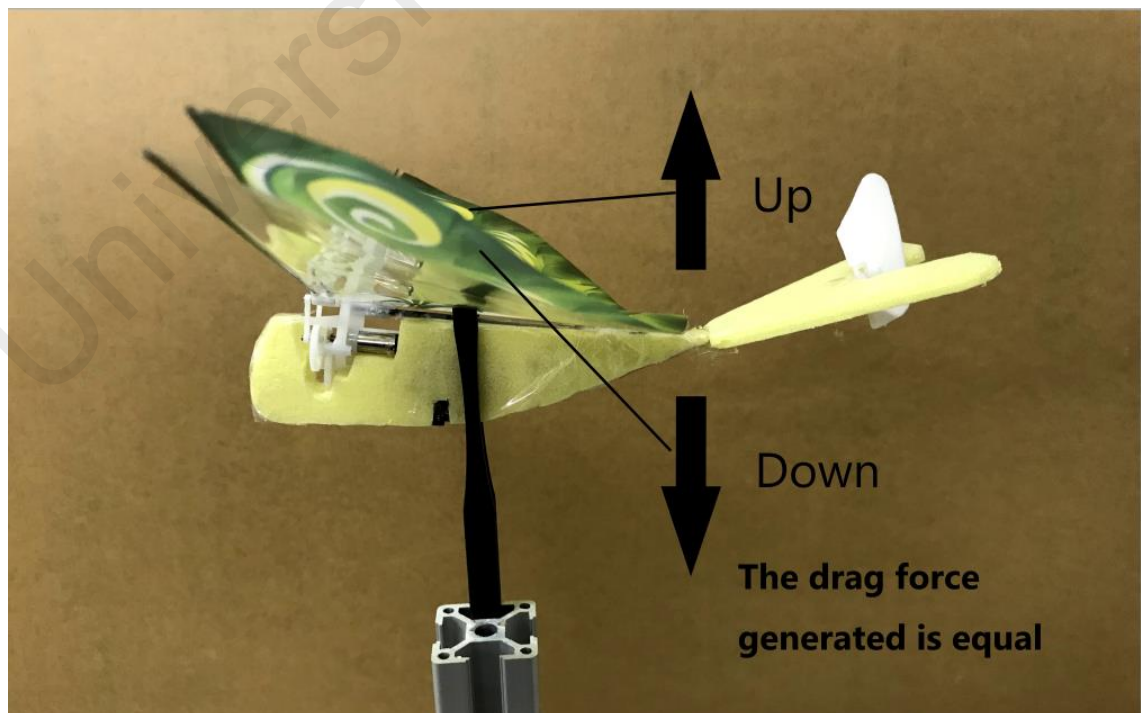


Figure 1.1 Flapping wing mechanism

1.3 Objectives

The objectives of this project are based on the development and research of flapping drone's wing component and as shown below.

- i. To analyze the one-way valve mechanism by using computation fluid analysis.
- ii. To design and develop a type of wings with one-way valve for flapping drone.
- iii. To investigate the performance of the flight.

1.4 Research Scope

This research consists of two parts--CFD simulation and actual experiment. The first part is the simulation of the influences of one way valves on flight performance based on ANSYS software. The second part is to make an actual flight test for models. Due to some limitations, the scopes of this research are as follow.

- i. Due to the lack of computer performance, CFD simulation only used 2D geometric model instead of 3D geometric model to improve the efficiency of the research process.
- ii. The flight test of the actual model can only be observed with human eyes. The flight height and velocity of the drone cannot be measured accurately.
- iii. Due to limited wing materials, only four types of wings are made for comparison.

1.5 Report outline

There are 5 chapters in this research report. Chapter 1 is the introduction of the flapping drone including the problem statement and objectives. Chapter 2 is the literature review of the previous study. Chapter 3 shows the methodology used for this one way valve mechanism study which has both computational fluid dynamic analysis and experiment.

Chapter 4 is the experiment and CFD result and comparison to verify the effectiveness of one way valve on the flapping wing. Chapter 5 summarizes the entire research report.

University of Malaya

CHAPTER 2: INTRODUCTION

2.1 Background

In 1903, the world's first aircraft which has the name “flyer” was built after thousands of test flights and hundreds of wind tunnel tests by the Wright brothers in the United States. The invention of the plane fulfilled the dream of mankind flying to the sky through machinery. With the development of technologies such as computers, lightweight materials, micro-electromechanical systems, sensors and high-energy batteries, conditions for the development of aircraft towards lighter, smaller and more flexible conditions have been formed (Zhou Jiping, 2004). In 1992, the Defense Advanced Research Projects Agency (DARPA) organized a seminar in Rand Corporation technologies that could revolutionize military operations in the next 20 years and outlined the research work required to implement a new military system based on new technologies. At the meeting, the experts first proposed the concept of micro aerial vehicles (MAVs) and believed that the micro aerial vehicles will have an impact on future military models. After the meeting, the U.S. government provided financial support to teams and universities working on micro air vehicles (Janson, 1995). With the next two years of evaluation and research, several research teams, including the Lincoln Laboratory, have reached a technical feasibility conclusion for the development of micro aircraft.

Researchers referred to the natural flying birds and insects in the design and manufacture of flapping wing aircraft by using the knowledge of bionics. Based on the observation of the flight status of birds which have high flight performance, It is found that the flapping wing has many advantages (Dornheim, 1998):

- i. The flapping wing can make a perfect combination of thrust and lift by flapping up and down with double wings. It can also make full use of unsteady air to get the best thrust and lift. And making the flight control time longer.
- ii. Flapping drones can take off and land without a runway.
- iii. The flapping-wing flight mode has high maneuverability, and it can quickly change the flight direction and flight speed by changing the flapping frequency.
- iv. The flapping flight has a special lift-generating mechanism and is the only flight mode that will not cause a stall.

Since the motion characteristics of flapping drone can achieve the goals that other aircraft cannot carry out, flapping drones have great use-value and prospects in the military and civilian fields. The usage of flapping drone in the

- i. Near-Earth flight reconnaissance: Satellites and spy planes can perform high-altitude reconnaissance very well. Due to their high distance from the ground, it is sometimes hard to clearly observe the condition on the ground. However, sending soldiers to conduct on-site investigations has a high-risk factor and long investigation time. The flapping drone is small and very flexible. It can freely shuttle through the urban building or jungle to obtain detailed battlefield information.
- ii. Electronic signal interference: Due to the small size of the flapping drone, it can avoid the enemy radar monitoring system. And interfere with the enemy's communication band at close range and implement electronic signal interference.
- iii. Hazardous environment detection: Carry out low-altitude detection of environments that are not suitable for human entry, and video images are transmitted in real-time.

- iv. Civil aspect: Outdoor terrain surveyors can use flapping-wing aircraft to carry equipment to survey terrain at low altitudes. And airports can use eagle-like flapping drones for airport airspace bird repelling missions.

2.2 Flapping mode

Birds have evolved through nature's species and possess a pair of flapping wings to adapt to free flight in the air. The flight style of birds is superior to the rotor and fixed-wing flight in many performance indicators. The flapping wing flight will not stall and can take off and land on the spot. The flight attitude changes quickly and has high maneuverability. According to observations, it is found that birds can change their flight attitude flexibly to adapt to different flight requirements during the flight in the air. Therefore, the aerodynamic problems encountered by birds are also variable. Birds can continuously fly in the air, which requires the bird's wings to generate lift during the flapping process to overcome gravity. And at the same time, it needs to generate a forward thrust to balance the air resistance in flight. Among the birds, only hummingbirds can hover in the air. Research experts have found that hummingbirds produce lift when flapping their wings, and they also generate lift on their wings with 75% lift and 25% lift when flapping (Ning, 2015). After the long-term evolution of natural species, the body structure of birds has evolved to be more conducive to flight. For example, the bones of birds are hollow, light and strong. Large and small airbags are distributed in the body to reduce the weight of birds. The primary and secondary feathers of the wings can cover and separated from each other. The feathers cover each other to increase the contact area with air during the upstroke, and it can increase the lift. The feathers open to create a gap to reduce the air resistance during the downstroke, thereby reducing the negative lift. Through the researcher's observation. The creatures that are flying in the air mainly include birds and insects. Although they all use the flapping-wing method, there is still a certain difference in their flight mechanism. Insects have smaller sizes. Their wings are

thin and light. And they have a certain degree of elasticity, Insects' beating frequency is higher (around 10~500Hz). Insects use one or two pairs of wings on the thoracic knuckle to flap up and down that allowing the wings to twist and swing to produce wingtip vortex. Then lift and thrust will be generated (Peng Bai, 2007). The wings of an insect are composed of two very thin membranes. It does not have muscles and bones which makes wings very light. According to research and analysis, the main chemical composition of insect wings is chitin which is very hard (Antonia B Kesel, 1998). Insect wings have crisscrossed wing veins on the surface which strengthen the wings. The insects mainly complete by changing the movement posture of the wings to control the speed and direction of the flight. However, some insects can control the flight by changing the position of the center of gravity. For example, a common dragonfly has a long abdomen, and the abdomen may be able to bend inwards during flight, thereby changing its center of gravity and changing its flying attitude.

There are many animals with superb flying skills in nature. And most of the animals use flapping wings to fly during the flight. Although flying creatures all adopt flapping-wing flight mode, due to individual differences between species, they have a flight attitude adapted to their respective bodies. Among them, flying animals of different body types, different types, and different living environments have different attitudes and flutter frequencies in the air; even if the size is similar, and the wings have different parameters, their flight attitudes are different. Flapping wing aircraft can produce higher lift when the Reynolds number is lower, so its size is highly miniaturized.

2.3 Overall design of flapping drone

California Institute of Technology, UCLA and AeroVironment Inc. for the DARPA TTO office have developed a principle prototype based on characteristics of bats with the name 'Microbat' (Matthew Keennon J. G., 2014). The first flight was successful in 1998. The air control time was only 9 seconds in the first flight. Later, the California institute improved it by installed skin with titanium alloy skeleton and used polymer film as the material of wings (Figure 2.1). At the same time, it also has a power transmission system combining the lever transmission mechanism and the gear reduction mechanism that made its maximum battery time extended to more than 20 minutes.



Figure 2.1 Microbat from California Institute of Technology.

In 1998, engineers and his team at the Georgia Institute of Technology in the United States developed insect-like micro aircraft called Entomopters (Figure 2.2) (RC Michelson, 1998). The two pairs of wings of this micro aircraft are like the wings of a butterfly. It plans to use the reciprocating chemical muscle as the power to drive the wings to flap.

The University of Brussels in Belgium has developed a hummingbird FWMAVs wing structure (Figure 2.3) (Y. Nan, 2015). Its wingspan is 90 mm, wing root is 25 mm and area of one wing is 1750 mm². Its wing is made by 15 micrometer thick polyester film.

The wing plane is equipped with two carbon fiber stiffeners which play a role in maintaining the plane geometry of the wings during flapping.

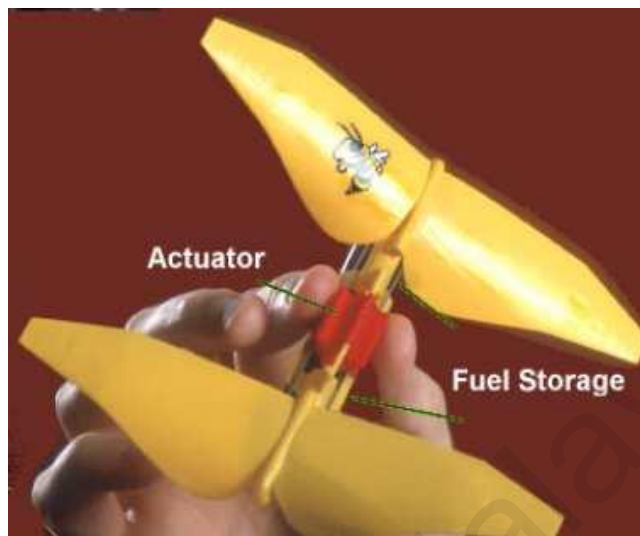


Figure 2.2 Entomopters from Georgia Institute of Technology

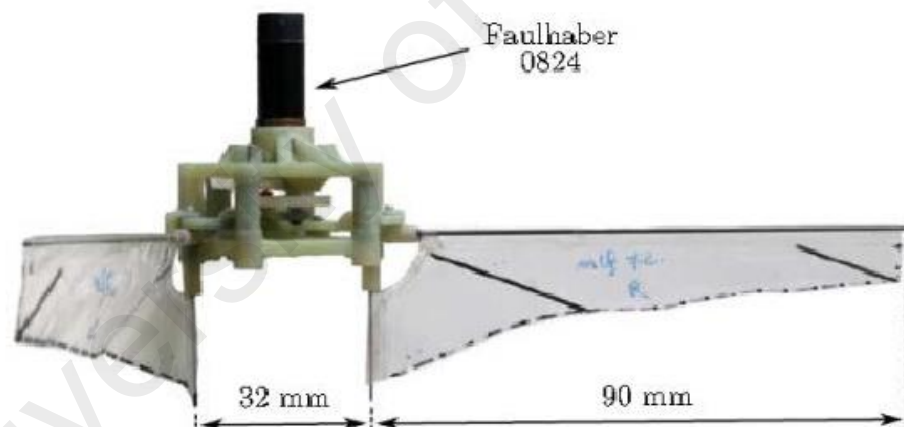


Figure 2.3 Hummingbird FWMAVs wing structure

Later, Quoc V Nguyen (2017) designed a flapping wing called FlowerFly at the National University of Singapore (Figure 2.4). It has two pairs of wings. And the area of each wing is 61cm^2 . It has the weight of 0.35 g and wingspan is 100 mm. Its wings are made by a different material which is called Myler film with 15 mm thickness. The wing leading edge and wing vein are composed of carbon rods with diameters of 0.8 mm and 0.3 mm respectively. In the subsequent experimental research, Quoc V Nguyen (2017)

analyzed and studied the effects of carbon rods with different diameters, the number of fin veins, and the arrangement angle of carbon rods on lift and energy consumption.



Figure 2.4 FlowerFly from National University of Singapore

2.4 Flapping Wings

In response to DARPA's call for research on Nano Air Vehicles (NAV), AeroVironment of the United States has researched a flutter-wing prototype "Nano Hummingbird". Since the first phase of design began in 2006, a total of about 300 wing patterns have been tested. Figure 2.5 shows some of the wing types which are made of different film materials, completely solid to high porosity, easy to stretch to highly reinforced, loose to relatively rigid. In addition to the different materials and shapes, the wings are equipped with carbon rods of different diameters as reinforcements (Matthew Keennon K. K., 2012).



Figure 2.5 Some wing types during NAV project implementation

In addition, there are many research institutions and scholars who have conducted design studies on the wings of FWMAVs. Wang (2013) used the Beta probability density function (BPDF) to approximately describe the shape of the wing and optimized its kinematics. He also parametrically expressed the position of the wing pitch axis and optimized for the design and analysis of the pitch axis position for four types of wings including rectangular wings, insect wings, quarter elliptical wings and delta wings. Grommem (2014) used B-spline curves to establish a geometric model of the wing and optimized the morphology. Ke (2017) based on an improved quasi-steady aerodynamic model to optimize the design of the geometric parameters and kinematic parameters of the wings under hovering. Shang (2009) proposed a novel manufacturing Lightweight, complex, centimeter-level wing technology. And he also designed several kinds of bionic wing mechanical performance experiments.

It is found that a negative peak of lift during upstrokes in the flapping rotary wing (FRW) generated instantaneous aerodynamics which counteracting the positive values

significantly (Zhou Jiping, 2004). Flapping drone also get same phenomenon because it has the same mechanism and kinetic of the FRW. Park (2004) found the method of birds to increase the efficiency of flight which is reducing the wind resistance by reducing area of feather on wings during upstrokes. Gao (2010) got inspired by this method and become the first researcher proposed a bore-hole design for flapping drone which is using the similar mechanism from birds. And this bore-hole design is effective for improving flight capability through experiment. Since there is no clear proof that bore-hole design can reduce air resistant during upstrokes. Later, Chen (2015) did a research on open a $25\text{mm} \times 15\text{mm}$ bore-hole on wings for a flapping drone. And it was found that bore-hole can increase the mean lift when the initial angle of attack is less than conversion angle of attack. He did the further research based on their previous study and found the mean lift increased up to 23% of maximum value (Long Chen, 2017). Figure 2.6 shows their model with borehole. His study is still only focus on the influence of a single borehole on flapping wing. Borehole still has the potential for research.

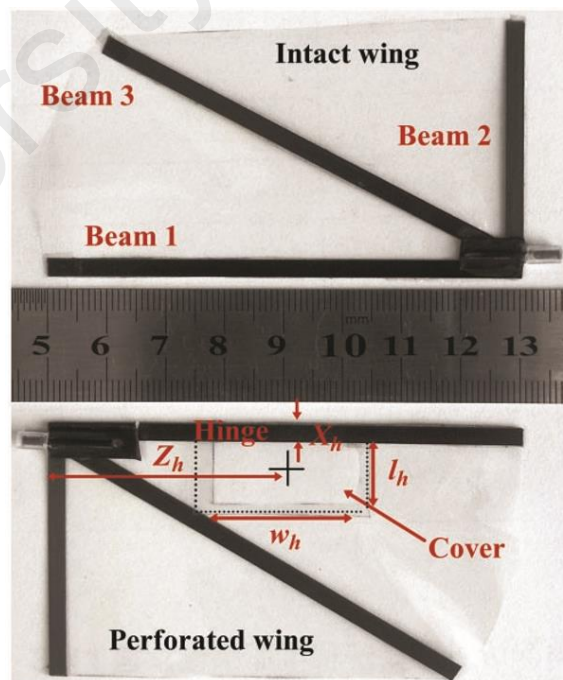


Figure 2.6 The intact and perforated wing test model from Long Chen (2015)

2.5 FWMAVs prototype

Since the 21st century, major research institutions around the world have increased their research on FWMAVs prototypes. This makes the development of FWMAVs very fast. Among the more representative research institutions are AeroVironment, Inc (USA), Festo (German), Temasek Laboratories and Delft University of Technology (Holland). Table 2-1 lists the representative FWMAVs from 2001 to 2015 (Quoc-Viet Nguyen, 2016).

Table 2.1 Representative FWMAVs

Name	Year	Span(cm)	Weight(g)	Hovering Nearly hovering
Microbat (Pornsin-sirirak T N, 2001)	2001	20	11.5	No
Mentor (Zdunich P, 2007)	2002	36	580	Yes
University of Delaware ornithopter (Madangopal R, 2005)	2005	36	15	No

Table 2.1 Continued

Name	Year	Span(cm)	Weight(g)	Hovering Nearly hovering
DelFly II (DELFLY, DELFLY, 2020)	2007	28	16	No
Van Breugel's FWMAV (van Breugel F, 2008)	2007	45	24	Yes
Harvard Robobee (Wood, 2007)	2007	3	0.06	Yes
Konkuk University FW-MAV (Park J H, 2008)	2007	15	8.7	No
DelFly Micro (Lentink D, 2009)	2008	10	3	No
University of Maryland FW-MAV (Mueller D, 2009)	2009	57.2	35	No

Richer' s FWMAV (Richter C, 2011)	2010	14.3	3.89	Yes
Wright State University FW-MAV (Hsu C K, 2010)	2010	20	12.56	No
Nano Hummingbird (AEROVIRONMENT, 2011)	2011	16.5	19	Yes
Festo Bionic-Opter (Mackenzie, 2012)	2012	63	175	Yes
Robotic-humming bird (ULB) (Karasek M, 2014)	2014	15	14	Yes
Tamkang University FW-MAV (Yang L J, 2015)	2015	20	9.62	No
NUS-TL FW-MAV (Nguyen Q V, 2015)	2015	22	16.6	Yes
DeFly Nimble (DELFLY, DeFly Nimble, 2018)	2018	33	29	Yes

Among these drones, most of bird-like aircrafts are like the Microbat from California Institute of Technology except for the hummingbird type (Matthew Keennon J. G., 2014). They have relatively low flapping frequency and amplitude. Since there is no rotation of the wings. This type of flapping drone produces lift only on flapping down.

Insect-like FWMAVs are different from bird-like ones in that their plane of motion is a near-horizontal plane. The flapping frequency of insect-like FWMAVs is relatively higher and flapping amplitude is also greater. The translation of the wing is accompanied by pitching or rotating movement. The existence of this compound motion results in a morphological change in the plane of the wing so that the aircraft can generate thrust in the vertical direction during the up and down strokes, thereby achieving low-speed flight or flying. Figure 2.7 shows the DeFly Explorer prototype developed by Delft University of Technology (C. De Wagter, 2014). It can hover in the air and is equipped with an

automatic navigation device weighing 0.98 grams and a stereo vision system of 4 grams, which can complete autonomous flight.

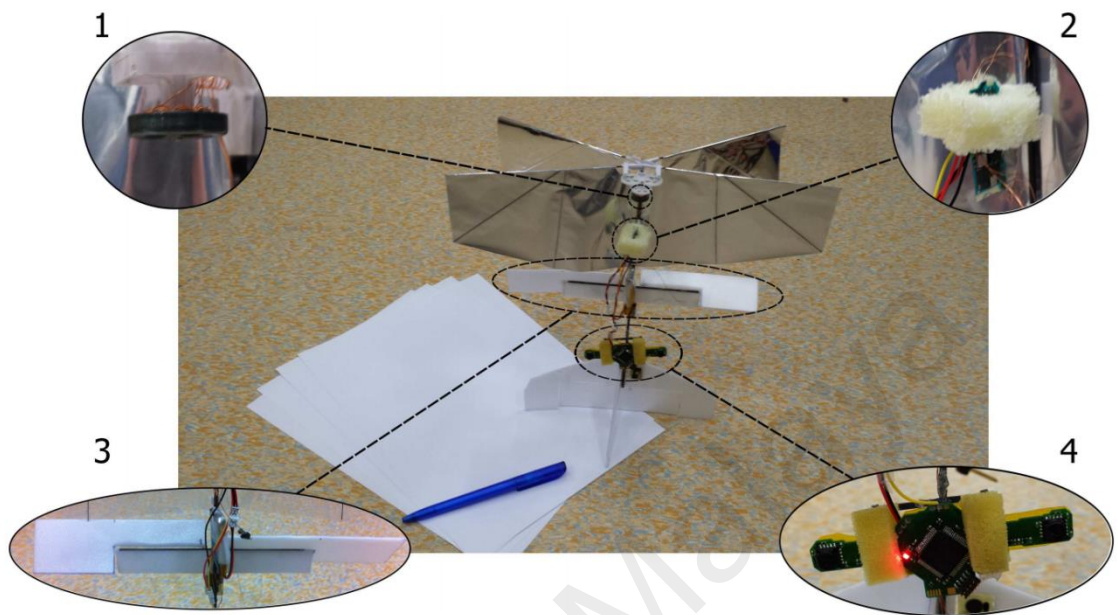


Figure 2.7 DelFly Explorer (1) Brushless motors (2) An autopilot with a complete IMU (3) Ailerons (4) The onboard stereo vision system

In addition to DelFly Explorer can achieved hover flight. AeroVironment's Nano Hummingbird (Matthew Keennon J. G., 2014), Brussel University's Robotic Hummingbird (Matěj Karásek, 2013), Festo's BionicOpter (Nina Gaissert, 2014) and other prototypes also can achieve hover flight (Quoc-Viet Nguyen, 2016).

2.6 Research gap

The previous study shows the different function and flight performance with different shape and wing size of the flapping drone. The research direction of most studies is to increase the lift and reduce the drag force of flapping wings by reducing the air resistance during upstrokes. Researchers have developed many wing methods to achieve this goal. German company Festo has developed a bionic flapping drone named SMART BIRD based on seagulls on 2012 which has two sections of wing and can fold the wings during flapping up to increase the performance (Wolfgang Send, 2012). Chen (2017) developed

the bore-hole on wings and verified the effect of bore-hole on increasing the lift. However, his research lacked a control group and did not study the principle of the borehole. The purpose of this research is to explore the principle of the one way valve and investigate its effectiveness of lift and drag.

University of Malaya

CHAPTER 3: RESEARCH METHODOLOGY

This research methodology chapter will introduce and describe the analysis of one way valve mechanism on the flapping wing in detail. The measure instruments, measurement and software also will be clarified.

3.1 Computer Fluent Dynamics

There is many current commercial fluid mechanics calculation software such as ANSYS FLUENT, ANSYS CFX, PHOENIX and STAR-CD. But ANSYS FLUENT software is the most widely used computational fluid dynamics software now. The numerical simulation calculation of wing motion is mainly to analyze the surrounding airflow filed during the periodical flapping of the wing in the air. The lift and drag force on the wing will be analyzed and calculated through the theorem of force interaction. In this research, fluid flow (fluent) method will be adopted. Figure 3.1 is a flow chart of the numerical simulation calculation of flapping wing motion in FLUENT.

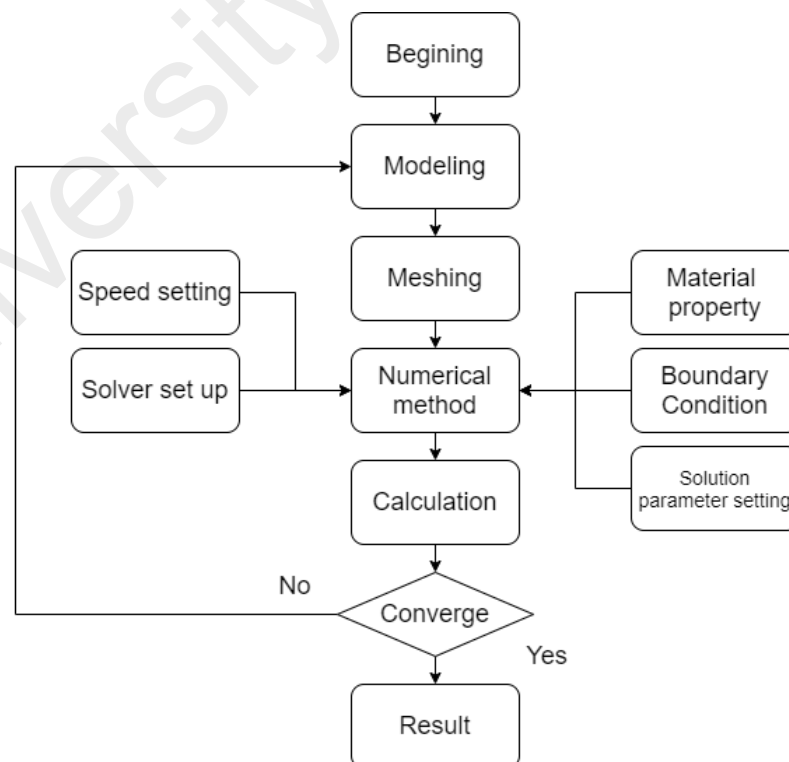


Figure 3.1 Flow chart of numerical simulation of wings motion

The following will introduce the setting steps in the numerical simulation process of the fluid problem of the one way valve mechanism by ANSYS software.

3.1.1 Geometry

Modeling is the first part of ANSYS and it is important. The computer fluent dynamics analysis part is focused on investigating whether the one way valve mechanism can increase the flight capability of the wing. Geometry will intercept the part of the wing around the one-way valve and valve itself. Because the structure and dimensions are relatively simple. It can adopt direct modeling method. This wind tunnel model will be directly made by design modeler in ANSYS workbench. According to the available materials of the flapping wing, set the wing thickness to 1 mm. Considering the rigidity and hardness of the plastic film, the length of the valve is set to 10mm. Figure 3.2 shows the remaining dimensions of the model.

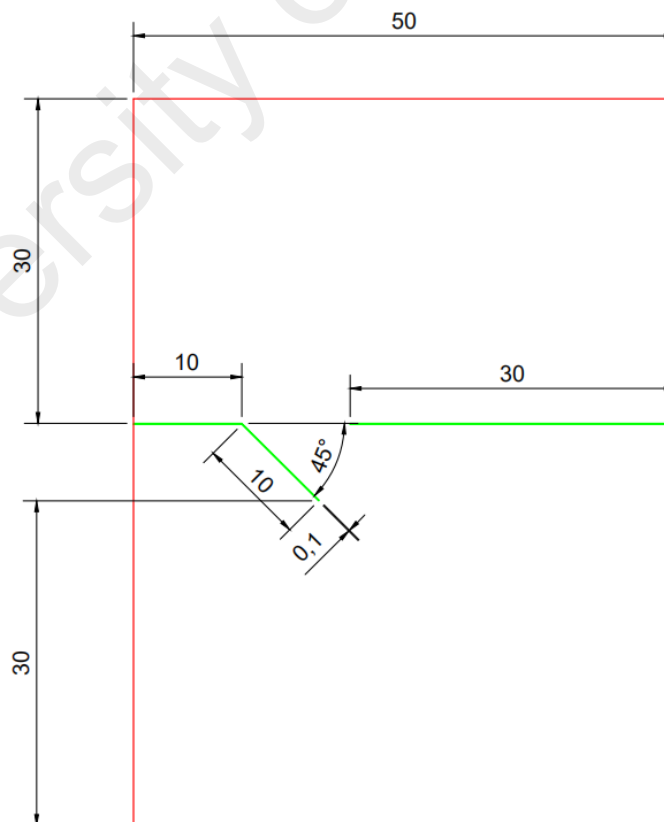


Figure 3.2 Dimensions of wind tunnel for one way valve mechanism

There are two parts of the body after extruding which are one way valve part and wind tunnel part. In the end, Boolean operation was used to combine these two parts.

Since the valve is a soft material, the opening and closing angles of the flapping drone are different during flight. The angle is between 0 to 45°. This experiment used four different angles for analysis. There are also two types number of valves--one valve and two valves to investigate the effects of one row and two rows. The dimensions of two valves wind tunnel shows as Figure 3.3.

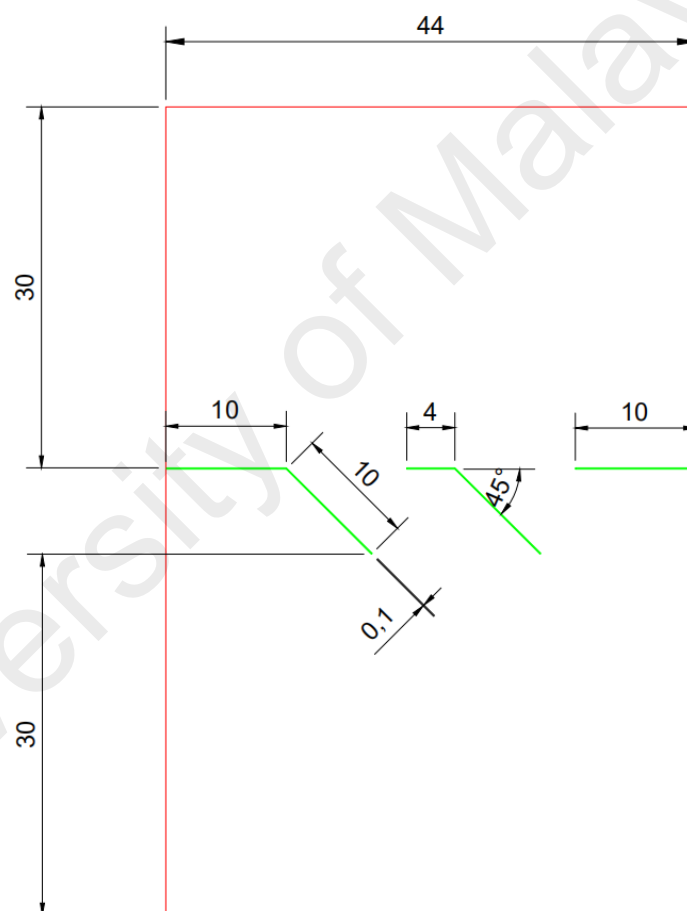


Figure 3.3 Dimensions of two valves wind tunnel

3.1.2 Meshing

The meshes form has a direct impact on calculation accuracy and calculation scale. The meshing method must be cautious. Since the model is relatively regular, the grid can be set as rectangle. To make the calculation of the valve and the vicinity of the wing more

accurate. Inflation control needs to be used on valve and wing structure, and the face sizing is used to control the size and number of the wind tunnel.

The transition ratio is 1.0, maximum layers are 6 and the growth rate is 1.2 for inflation, and the element size is set to 0.5 mm. The total elements about the model are 25846. The model has two types of inlets. The first type is all inlet is above the wing. The second type has one extra inlet below the wing. Figure 3.4 and figure 3.5 shows the style of meshing and two types of inlets and outlets of fluid.

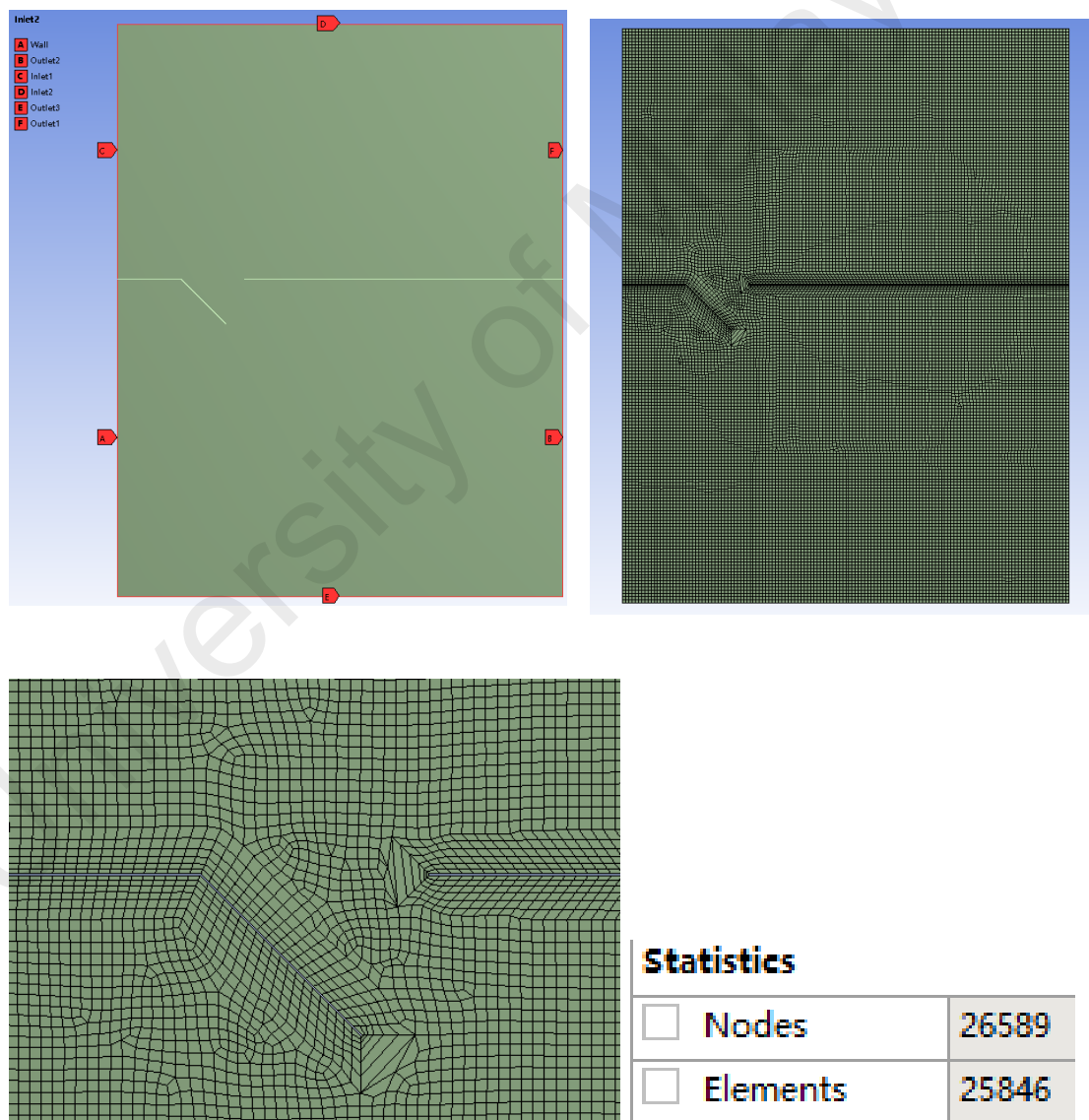


Figure 3.4 One valve at 45 degrees with 2 inlets

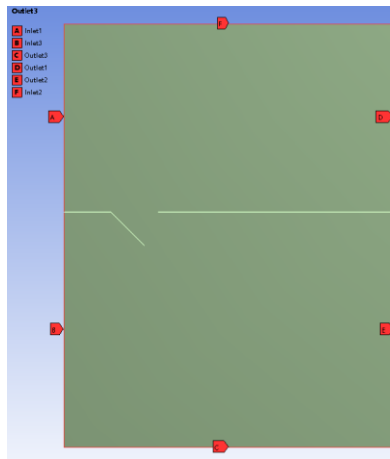


Figure 3.5 One valve at 45 degrees with 3 inlets

Next is the meshing of the two valves. The meshing control method is same with one valve model. And the total elements are 11798. Figure 3.6 and figure 3.7 shows the meshing and two types of inlets and outlets.

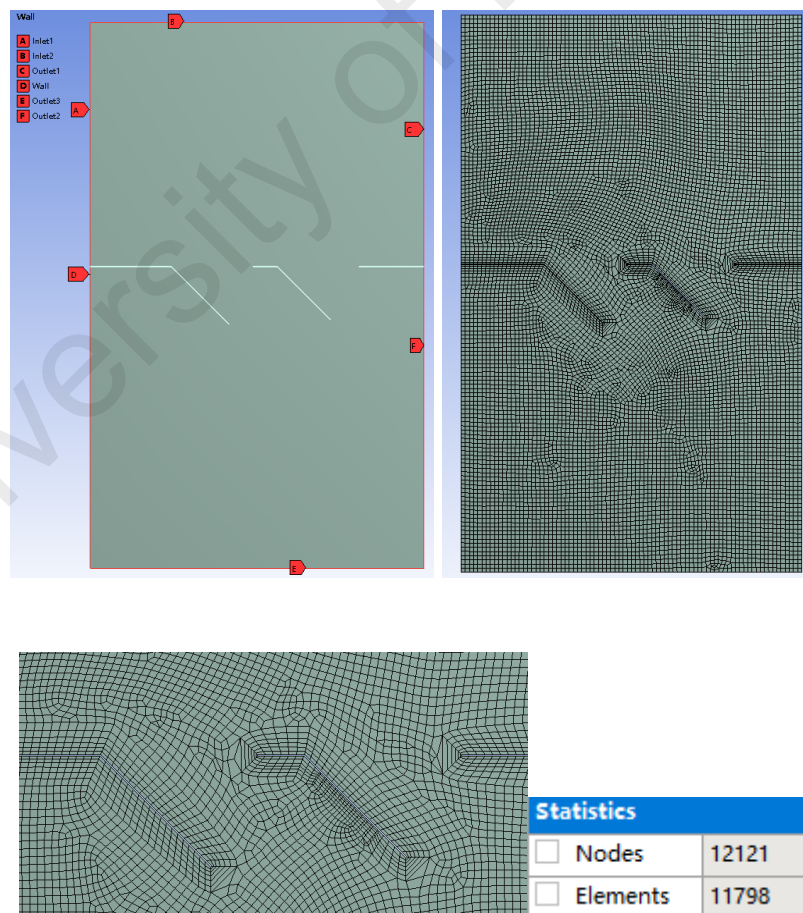


Figure 3.6 Two valves at 45 degrees with 2 inlets.

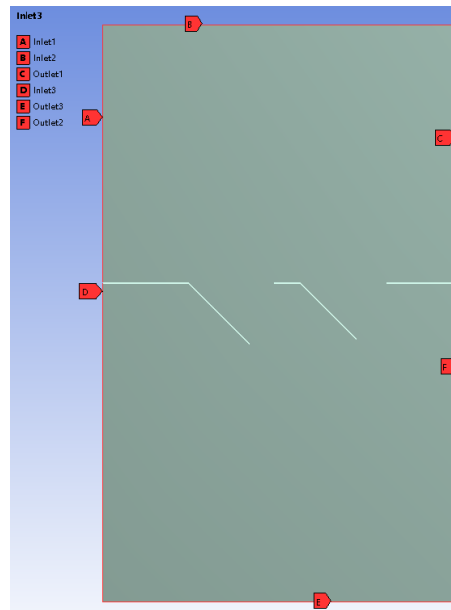


Figure 3.7 Two valves at 45 degrees with 3 inlets

3.1.3 Governing equation – continuity and momentum

The movement of any fluid must follow the three conservation laws of nature which are conservation of mass, conservation of momentum and conservation of energy. These three conservation laws are embodied in fluid mechanics as continuity equation, momentum equation and energy equation.

First, it will be introduced that the embodiment of conservation of mass in the flow which is the continuity equations. It means that the quality that flows into the control unit at a certain time interval is equal to the quality that flows out of the control unit during that time. Its differential equation is expressed as follows (Jiaqing, 2014).

$$\frac{\partial \rho}{\partial t} + \frac{\partial(\rho u)}{\partial x} + \frac{\partial(\rho v)}{\partial y} + \frac{\partial(\rho w)}{\partial z} = 0 \quad \text{Equation 1}$$

Where ρ - fluid density (kg/m^3), t - time (s), u , v , w - the component of the fluid velocity in the x , y , z axis direction (m/s)

As for incompressible flow problem for constant flow. Since $\frac{\partial \rho}{\partial t} = 0$, the continuity equation can be written as:

$$\frac{\partial u}{\partial x} + \frac{\partial v}{\partial y} + \frac{\partial w}{\partial z} = 0 \quad \text{Equation 2}$$

Then introduce the embodiment of the law of conservation of momentum in the flow problem which is Navier-Stokes equation (N-S equation). Its essential meaning is the embodiment of Newton's second law in fluid motion. It means that the composition of forces of all external forces on a fluid unit is equal to the rate of change of the momentum of the fluid unit over time. The differential expression of the equation in the three directions of x, y and z can be written as follows.

$$\frac{\partial(\rho u)}{\partial t} + \text{div}(\rho u \vec{u}) = -\frac{\partial(\rho)}{\partial x} + \frac{\partial(\tau_{xx})}{\partial x} + \frac{\partial(\tau_{xy})}{\partial y} + \frac{\partial(\tau_{xz})}{\partial z} + F_x \quad \text{Equation 3}$$

$$\frac{\partial(\rho v)}{\partial t} + \text{div}(\rho v \vec{u}) = -\frac{\partial(\rho)}{\partial y} + \frac{\partial(\tau_{xy})}{\partial x} + \frac{\partial(\tau_{yy})}{\partial y} + \frac{\partial(\tau_{yz})}{\partial z} + F_y \quad \text{Equation 4}$$

$$\frac{\partial(\rho w)}{\partial t} + \text{div}(\rho w \vec{u}) = -\frac{\partial(\rho)}{\partial z} + \frac{\partial(\tau_{xz})}{\partial x} + \frac{\partial(\tau_{yz})}{\partial y} + \frac{\partial(\tau_{zz})}{\partial z} + F_z \quad \text{Equation 5}$$

Where p - the pressure of the fluid unit (Pa), $\tau_{xx}, \tau_{xy}, \tau_{xz}$ - the component of the viscous force on the fluid element unit surface(Pa), F_x, F_y, F_z - the volume force of the fluid unit in the x, y, and z directions.

The last equation is the embodiment of the law of conservation of energy in the flow problem-energy equation. It means the increase rate of the energy contained in the fluid microcell and the net heat flux entering the fluid microcell plus the amount of work done by the mass force and surface force on the fluid microcell. It can be expressed as follows.

$$\frac{\partial \rho E}{\partial t} + \text{div}[u(\rho e + \rho)] = \text{div} \left[k_{eff} \text{div} T - \sum_j h_j J_j + (\tau_{eff} * u) \right] + S_h \quad \text{Equation 6}$$

Where E- energy of fluid unit including kinetic energy, potential energy and internal energy (J/kg), h- enthalpy (J/kg), k_{eff} - effective thermal conductivity (W/(m*K)), J_j - diffusion flux, S_h - volume heat source term including chemical reaction heat.

The research on the aerodynamic performance of the one way valve wing in this paper is an incompressible flow problem and the heat exchange can be ignored. Therefore, only the first two conservation laws (conservation of mass and Navier Stokes equation) are involved in the subsequent numerical simulation calculations and the energy equation is not included.

3.1.4 Properties/Numerical method

The flight dynamics of insects are affected by the Reynolds number scale. The formula for calculating the average Reynolds number during the flight Re_f as follow (Wei Shyy, 1999).

$$Re_f = \frac{4\phi f l^2}{v_1 AR} \quad \text{Equation 7}$$

Where ϕ - flapping amplitude of wings, f - flapping frequency (Hz), l - span length (m), v_1 - kinematic viscosity of fluid (m²/s), AR- aspect ratio.

Aspect ratio is the ratio of the span length to the wing area. At the same time, AR also showed the relationship between chord length and wingspan length. The higher the ratio of wingspan to chord, the greater the aspect ratio. However, an excessively large aspect ratio represents an excessively long wingspan, and the moment at both ends of the wing is too large during the flapping process. The carbon rod responsible for the transmission

may be deformed or broken during flight. Thus the most reasonable wing aspect ratio should be between 1 and 2. The formula for calculating aspect ratio is showed as follow (Wei Shyy, 1999).

$$AR = \frac{l^2}{S} \quad \text{Equation 8}$$

Where l - span length (m) and S – wing area.

The dimension of wing and parameter of flapping is showed as follow. Amplitude of flapping \emptyset is between $90^\circ \sim 120^\circ$. According to the real model, the span length is assumed to be 28 cm. The amplitude of flapping is 90° and maximum flapping frequency is 10 Hz. The temperature of air is considered as general indoor temperature which is 25°C . The kinematic viscosity of air is 1.562×10^{-5} under 25°C . Because the length of carbon rod and the distance between two fixed points are fixed. The chord length only can be designed around 9 cm. Therefore, the wing area is about 761.7 cm^2 . The aspect ratio is 1.029 by calculation. The Reynolds number during flight is equal to 4877.75 is calculated by equation 7. For flow over a plane, transition from laminar to turbulent begins at about $Re \cong 1 \times 10^5$ (Yunus A.Çengel, 2015). This Reynolds number of the wing is much smaller than 10^5 . Thus, the laminar method will be considered for subsequent calculations in viscous.

At the same time, computer fluid dynamic is used to analysis the one way valve mechanism on wings. Therefore, the Reynolds number of the valve also need to be calculated. The calculation equation as follow (Yunus A.Çengel, 2015).

$$Re_v = \frac{\rho VL}{\mu} = \frac{\mu L}{V} \quad \text{Equation 9}$$

Where μ - dynamic viscosity of fluid (kg/m-s), V - flow speed of fluid (m/s), L - thickness of one way valve (m).

In this research, the dynamic viscosity of air is 1.849×10^{-5} kg/m-s and the density of air is 1.184 kg/m³ when the temperature is 25°C . The current speed of MAV is about $20\sim 60$ km/h (5.6 m/s ~ 16.7 m/s). According to the measurement of the prototype, the speed of flight is about 6 m/s that is eligible. The speed of flight is used for flow speed. The thickness is 1×10^{-3} m. After calculation, the Reynolds number of the valve Re_v is equal to 384 which is also smaller than 10^5 . From Re_f and Re_v it can be confirmed the laminar method should be used.

At the same time for the rigor of the experiment. The flow around the wing needs to be considered. Therefore, it is necessary to make a comparison group using the transition SST method. The transition SST model is widely used in the viscous simulation. It combines the k-epsilon in free flow with the k-omega model near the wall (Takasi Misaka, 2006). Therefore, it is most accurate when solving the flow close to the wall. And transition SST model is very suitable for solving wing airflow.

The following describes the setting steps of FLUENT software in the process of numerical simulation of fluid problems. First, single precision solver is chosen for this case. Two models are used in viscous that are laminar and transition SST. The simulation does not involve energy, so turn off the energy option. The fluid is air and its density is set to 1.184 kg/m³ and viscosity is set to 1.849×10^{-5} kg/m-s. Next will show the setup in the boundary condition. It includes the determination of the fluid matter in the calculation area, the determination of outlet boundary conditions and inlet boundary conditions, and the determination of wall boundary conditions, etc. Inlet 1 and inlet 3 have the same speed that is 6 m/s and inlet 2 at the top of the wind tunnel is 1 m/s. The fifth step is to set and control the solution method. This step includes the setting of the solution parameters. The

SIMPLE solution method is used in this analysis. Then Initialize from entry boundary conditions and start to run iterative calculation. The last step is the post-processing of the calculation results and display velocity streamline and pressure contour in the result. Then optimize the result.

The aerodynamic characteristics of the wing can be characterized by the lift characteristic coefficient and the drag characteristic coefficient. They are all dimensionless numbers. The calculation formulas of instantaneous drag coefficient C_d and instantaneous lift coefficient C_l are as follows (ToolBox, 2010).

$$C_l = \frac{L}{\frac{1}{2}\rho v^2 S} \quad \text{Equation 10}$$

$$C_d = \frac{D}{\frac{1}{2}\rho v^2 S} \quad \text{Equation 11}$$

Where L- lift force (The lift force is perpendicular to the direction of the airflow velocity and the direction is upward), D- drag force (Resistance is in the same direction as the incoming flow velocity and is positive backward), v- the velocity of the airflow to the object, ρ - fluid density, S- wing area.

Another parameter that is relatively important for analyzing the function of the one way valve is the mass flow rate. It shows the mass of liquid passing the area per unit time. It can generally be used to verify the correction of meshing and setup by calculating the difference of mass between inlets and outlets. At the same time, the mass of fluid passing through the valve can also be calculated. The mass flow rate at any flow section is expressed as follows (Yunus A.Çengel, 2015).

$$m = \rho VA \quad \text{Equation 12}$$

Where A- cross section area (m^2).

This research will use ANSYS Fluent to calculate two types of one way valves mechanism and different angles to obtain a series of lift coefficient, drag coefficient and mass flow rate data, and then compare the data.

3.1.5 Simulation cases

Since the valve will be tested at four opening angles which are 3° , 15° , 30° , 45° , the total number of models is 8 in this case.

There are two types of simulation cases in this CFD analysis. The first is that there is only one valve on the wing and the second type is two valves on the wing. Since the angle range of the one way valve is between 0 to 45° , each type of case will be calculated using four angles that are 3° , 15° , 30° , 45° , and the number of inlets also will be set to 2 types. The viscous model will be adopted both laminar and transient SST. The rest of the settings remain the same. There are 32 cases in total. Finally, this research utilizes the cases to compare and verify the improvement of the one-way valve on the wing and determine the mechanism on the experimental model.

3.1.6 Mesh dependency investigation and validation

The analysis result of computational fluid dynamic solution is not completely credible unless it can be proved that the calculation result depends on meshing or using experimental data for comparison. The results from coarse mesh and dense mesh can never be the same. Therefore, the meshing of the grid plays an important role in CFD analysis. In this research, it is necessary to vary the mesh to get an acceptable level of tolerance. The one valve at the 45-degree model with 3 inlets will be used for the mesh dependency test as a standard for all models in this research because it has both inflation and face sizing in meshing of the grid. The influence of both methods on meshing and

results will be considered in this part. Table 3.1 shows the mesh elements and drag force under different element sizes. Figure 3.8 shows the relationship between mesh elements and drag force where x-axis is the drag force and y-axis are the mesh elements.

Table 3.1 Mesh dependency test on element size

	Inflation Maximum Layers	Face Sizing Element Size [mm]	Mesh Elements	Drag-Force [N]
DP1	6	2.5	486	0.42773163
DP2	6	2	947	0.52073113
DP3	6	1.5	1444	0.50215045
DP4	6	1	2932	0.45776061
DP5	6	0.9	3500	0.43601853
DP6	6	0.8	4534	0.41672582
DP7	6	0.7	5833	0.41595792
DP8	6	0.6	7698	0.41016532
DP9	6	0.5	11798	0.40938259
DP10	6	0.4	17739	0.34243033

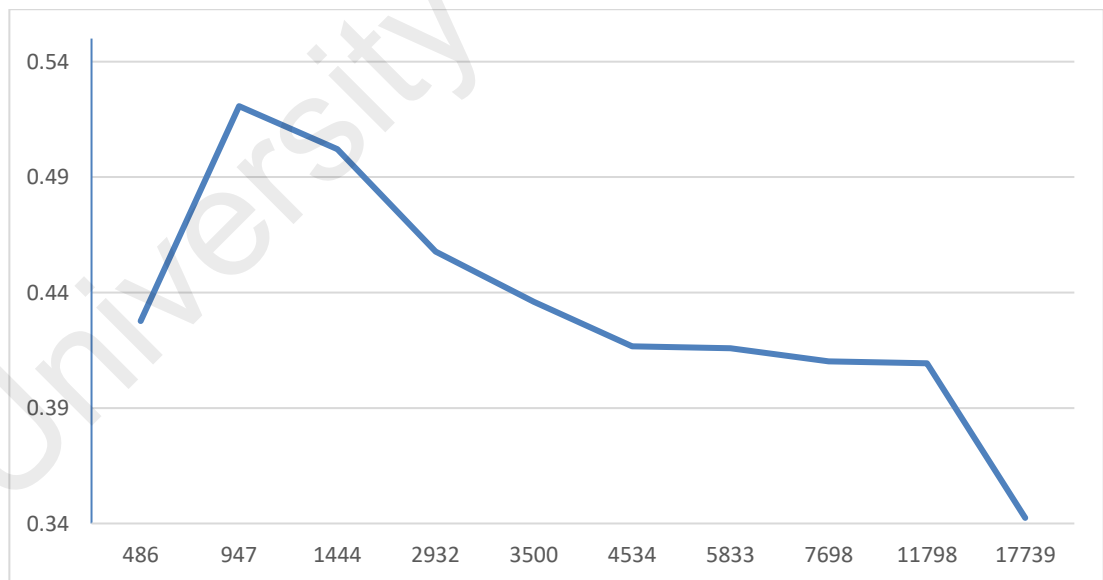


Figure 3.8 Line chart of drag force under different mesh elements

It is clear to see the drag force is increasing when the element number is smaller than 1000 and after that, the drag force shows a slight decrease until after 12000. After more than 12000 elements, the decreasing trend is palpable. The most stable range in the entire

graph is between 4500 and 12000. That means the 0.5 mm element size in this analysis is reasonable.

Another parameter is inflation maximum layers that also need to be verified. Investigation of inflation layers will be divided into ten groups, from the least one layer to the most ten layers. Another variable element size is fixed at 0.5mm. Table 3.2 shows the detail of the mesh dependency test.

Table 3.2 Mesh dependency test on inflation layers

	Inflation Maximum Layers	Face Sizing Element Size [mm]	Mesh Elements	Drag-Force [N]
DP1	1	0.5	11223	0.42005849
DP2	2	0.5	11182	0.40789107
DP3	3	0.5	11117	0.41341439
DP4	4	0.5	11464	0.40852656
DP5	5	0.5	11497	0.40842073
DP6	6	0.5	11798	0.40938259
DP7	7	0.5	11846	0.4117105
DP8	8	0.5	11881	0.42813918
DP9	9	0.5	11936	0.41876263
DP10	10	0.5	11927	0.42160288

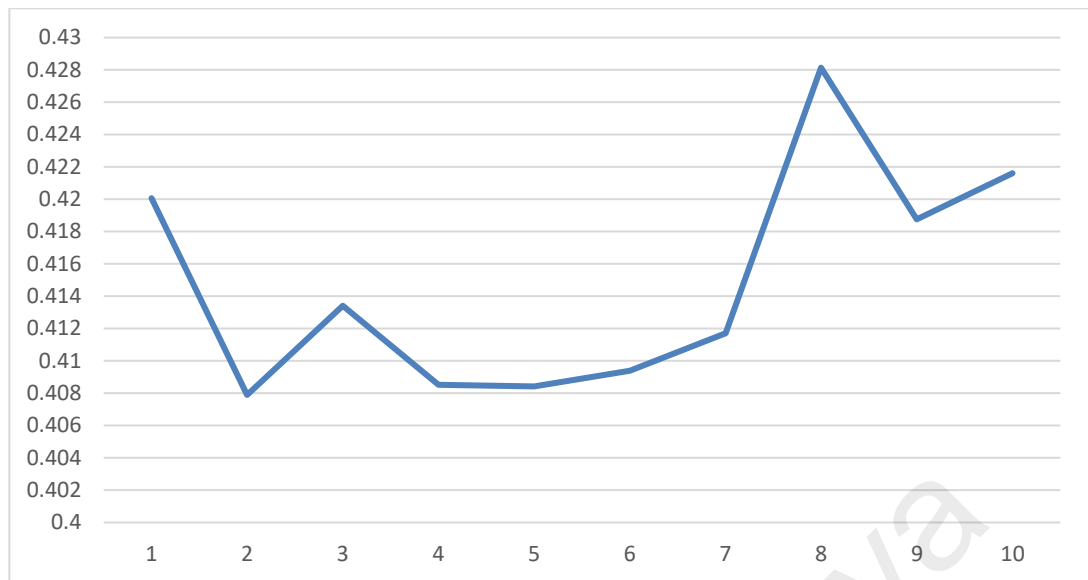


Figure 3.9 Line chart of drag force under different inflation maximum layers

It can be observed that the drag force stabilizes between 4 layers and 7 layers. The drag force increases rapidly after inflation layers more than 7. The average number of inflation layers 5 is taken from the stable range.

3.2 Experimental model and measurement method

3.2.1 Materials

According to the calculation, the power of the flapping drone's motor is only 15 W. The weight of the flapping drone is usually very light, and the wings must be made of thin and light materials. At the same time, in order to imitate the wing shape of birds, it is necessary to make the wing above and below the wing concave in flight to reduce the negative lift on the flight and increase the downward swing. Overall, the wing material of the bionic wing requires corrosion resistance, softness, toughness, and ability to withstand high frequency beating without failure. Therefore, the available materials usually are nylon silk, brocade silk, non-woven fabric and plastic film. Among them, plastic film is soft, strong, corrosion-resistant and easy to process. Therefore, polyethylene, polyvinyl chloride, polyester and polyimide can be chosen for producing wings. Tale 3.3 shows the comparison of the parameters of several typical plastic film

materials (CURBELL PLASTIC, 2020). Finally, Mylar film is a type of polyester selected as the material of the wing, due to its good mechanical and chemical properties, small thickness and easy to obtain. Mylar film is widely used as a material on flapping drone especially on insect-like MAV wings (Lu, 2018). The density of Mylar is 1390 g/mm³ and tensile strength is 34000 psi (Grafix, 2020). Young's modulus is 602–1400 MPa (Lu, 2018).

Table 3.3 The parameters of several typical plastic film materials

	Polyethylene (PE)	Polyvinyl chloride (PVC)	Polyester film (PETP)	Polyimide (PI)
Density (g/mm ³)	910-925	1300-1580	1370-1380	1340-1600
Elastic Modulus (GPA)	7-24	45-50	57	80-100
Tensile Strength (MPA)	0.12-0.95	3.3	2.8	2.8
Elongation (%)	60-650	20-40	50-300	70-150

3.2.2 Shape

Figure 3.10 shows the structure and a planform view of the flexible membrane wing developed. The main parts of the wing are the ribs and the skin. The wing's cover shape is segment area of circle with span length of 280mm and height of 90 mm radius of 156 mm that is made by 0.1 mm thick Mylar film, which is a strong, lightweight and thin polyester film (shown in Appendix A). The Mylar sheet is stiffened by carbon-fibber rods with diameter of 2 mm and length of 130 mm as shown in Appendix A. The main rods construct the leading edge of the wing and provide the wing's stiffness which lead the flapping of wings.



Figure 3.10 The structure and a plan form view of the wing

3.2.3 Model

After the shape of the wing is designed, the next step is to design the one way valve on the wing. In this design, a variety of methods were used to set the one-way valve on the wing. A total of three types of wings have been designed. The first one is used one way valves to cover the entire wing surface. The second type is to install one row of valves in the front section of the wing. The last one is also used one row of valves. The difference between the second and third types is the valve direction that is divided into forward and backward. Figure 3.12 shows three types of experimental wing models. The one way valve has two parts. The first part is the valve which can also be called as loose leaf which can open and close to release the wind when upstroke. Another part is the open hole on the wing which can let the air goes through the valve. Figure 3.11 shows the tools for making flapping wings. The needle is utilized to make holes on the wings. A utility knife is utilized to cut valves.

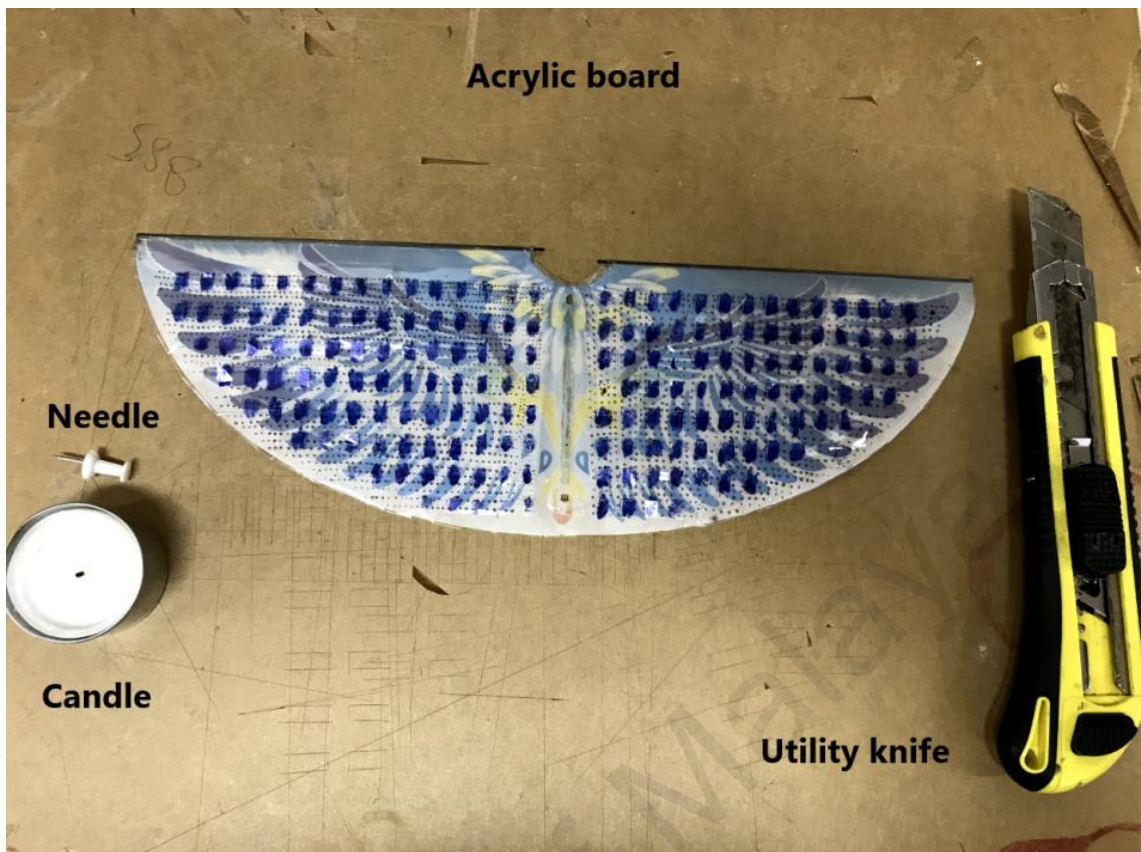


Figure 3.11 Tools for making wings



Figure 3.12 Three types of experimental model

3.2.4 Measurements and instruments

The GM8903 hot wire anemometer was used to measure the wind speed by flapping of wing. This anemometer measures wind speeds in the range of 0~30 m/s and has a resolution of 0.1 m/s.



Figure 3.13 Hot wire anemometer

Most of the airflow generated by the wings of a flapping drone is behind and below the wings. To accurately measure the velocity of airflow from flapping wings, a measurement plan based on the wing shape is designed. Figure 3.15 shows the measurement using anemometer. There are four plans distributed above, below and at the gravity center of the drone body which can well cover the area where the wing generates wind speed. The center of gravity is the origin of the coordinate axis. The distance between each measuring point is 100 mm. To avoid the uncertainty of the maximum wind speed direction during manual measurement, the measurement direction of each point adopts the y-axis direction and the z-axis direction. Figure 3.14 shows the measurement process.



Figure 3.14 Measurement of velocity generated by wings

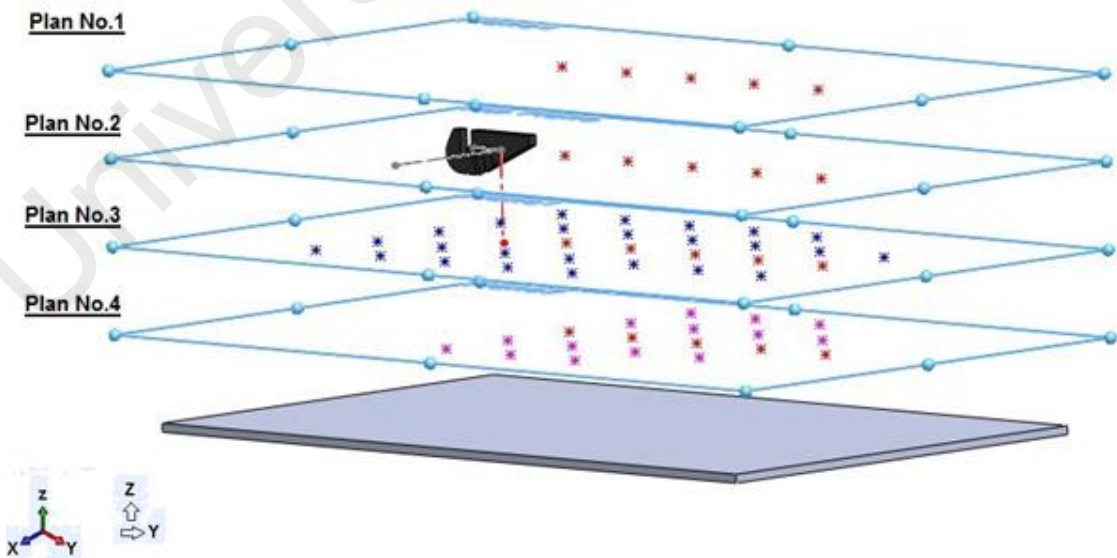


Figure 3.15 The design points for measuring the velocity profile

CHAPTER 4: RESULTS & DISCUSSION

4.1 CFD results

4.1.1 Mass flow rate

The mass flow rate shows the proportion of air passing through the one-way valve in different models and verifies the credibility of the results. Figure 4.1 to Figure 4.4 shows the sketch of two types one way valve mechanism with two types of inlets which can divide into four types and named from type 1 to type 4. The laminar model and the transition SST model were both used for calculation. There are four parts that shows the details of the mass flow rate at different valve angle.

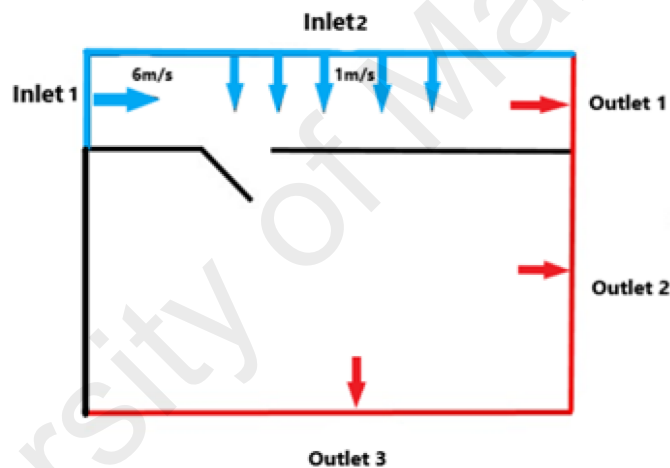


Figure 4.1 Single valve with 2 inlet (type 1)

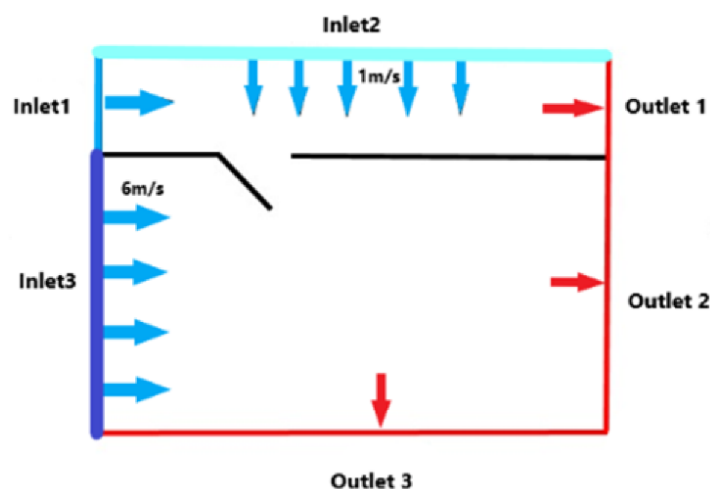


Figure 4.2 Single valve with 3 inlets (type 2)

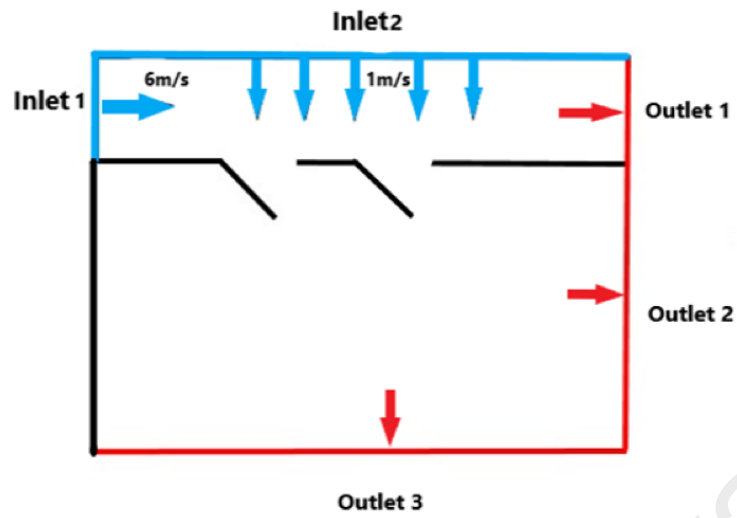


Figure 4.3 Double valves with 2 inlets (type 3)

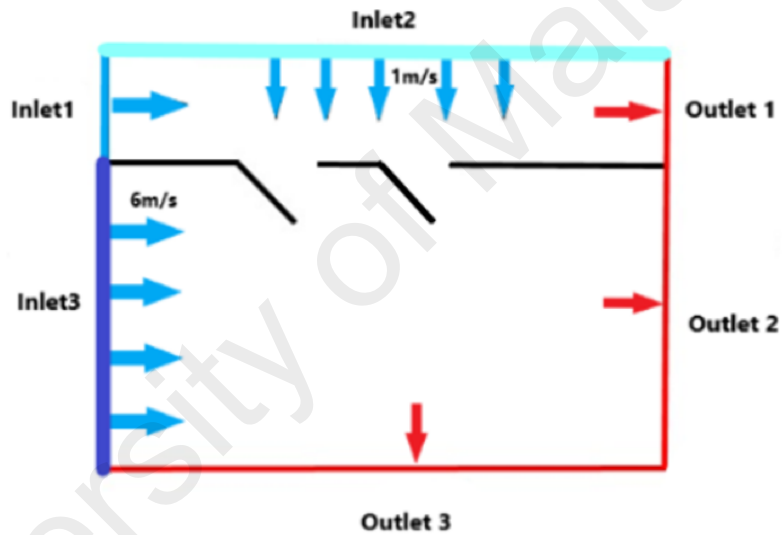


Figure 4.4 Double valves with 3 inlets (type 4)

4.1.1.1 Single valve with laminar model

This part shows the mass flow rate and percentage of air going through the valve from 45 degrees to 3 degrees of type 1 and type 2 laminar model. It is observed that the greater the opening angle of the valve, the greater the percentage of air go through the valve when there are only two inlets. However, the percentage of air goes through the valve became maximum when the angle of the valve is 30 degrees.

Table 4.1 Mass flow rate of single valve at 45 degrees with 2 inlets

One valve with two inlets	Name	Mass Flow Rate	Absolute
	QInlet-1	0.29400006	0.29400006
	QInlet-2	0.085749969	0.085749969
	QOutlet-1	-0.3319532	0.3319532
	QOutlet-2	0.017886138	0.017886138
	QOutlet-3	-0.06568291	0.06568291
	QInlet-total	0.047796829	0.379750029
	Qoutlet-total	-0.047796772	0.047796772
	Mass conversion	$Q_{in} - Q_{out}$	5.7742E-08
	Percentage go into valve	$(Out2+out3)/(In1+In2)$	12.58637745
	Percentage not go into valve	$(Out1)/(In1+In2)$	87.41360754
		Total	99.99998499

Table 4.2 Mass flow rate of single valve at 30 degrees with 2 inlets

One valve with two inlets	Name	Mass Flow Rate	Absolute
	QInlet-1	0.29400006	0.29400006
	QInlet-2	0.085750043	0.085750043
	QOutlet-1	-0.34079024	0.34079024
	QOutlet-2	-0.024587592	0.024587592
	QOutlet-3	-0.014372199	0.014372199
	QInlet-total	0.379750103	0.379750103
	Qoutlet-total	-0.379750031	0.379750031
	Mass conversion	Qin - Qout	7.2E-08
	Percentage go into valve	$(\text{Out2}+\text{out3})/(\text{In1}+\text{In2})$	10.25932335
	Percentage not go into valve	$(\text{Out1})/(\text{In1}+\text{In2})$	89.74065769
		Total	99.99998104

Table 4.3 Mass flow rate of single valve at 15 degrees with 2 inlets

One valve with two inlets	Name	Mass Flow Rate	Absolute
	QInlet-1	0.29400006	0.29400006
	QInlet-2	0.085750043	0.085750043
	QOutlet-1	-0.35686108	0.35686108
	QOutlet-2	-0.029048113	0.029048113
	QOutlet-3	0.006096025	0.006096025
	QInlet-total	0.379750103	0.379750103
	Qoutlet-total	-0.379813169	0.379813169
	Mass conversion	Qin - Qout	-6.3065E-05
	Percentage go into valve	$(\text{Out2}+\text{out3})/(\text{In1}+\text{In2})$	6.043997966
	Percentage not go into valve	$(\text{Out1})/(\text{In1}+\text{In2})$	93.97260914
		Total	100.0166071

Table 4.4 Mass flow rate of single valve at 3 degrees with 2 inlets

One valve with two inlets	Name	Mass Flow Rate	Absolute
	QInlet-1	0.29400003	0.29400003
	QInlet-2	0.085750043	0.085750043
	QOutlet-1	-0.37623957	0.37623957
	QOutlet-2	-0.005599796	0.005599796
	QOutlet-3	0.002089346	0.002089346
	QInlet-total	0.379750073	0.379750073
	Qoutlet-total	-0.37975002	0.37975002
	Mass conversion	Qin - Qout	5.28E-08
	Percentage go into valve	$(\text{Out2}+\text{out3})/(\text{In1}+\text{In2})$	0.924410672
	Percentage not go into valve	$(\text{Out1})/(\text{In1}+\text{In2})$	99.07557542
		Total	99.9999861

Table 4.5 Mass flow rate of single valve at 45 degrees with 3 inlets

One valve with three inlets	Name	Mass Flow Rate	Absolute
	QInlet-1	0.294	0.294
	QInlet-2	0.085750014	0.085750014
	QInlet-3	0.36749995	0.36749995
	QOutlet-1	-0.34588832	0.34588832
	QOutlet-2	-0.30694866	0.30694866
	QOutlet-3	-0.094412953	0.094412953
	QInlet-total	0.379750014	0.379750014
	Qoutlet-total	-0.747249933	0.747249933
	Mass conversion	Qin - Qout	7.4506E-08
	Percentage go into valve	$(\text{Out2}+\text{Out3}-\text{In3})/(\text{In1}+\text{In2})$	8.916829954
	Percentage not go into valve	$(\text{Out1})/(\text{In1}+\text{In2})$	91.08316188
	Total	99.99999184	

Table 4.6 Mass flow rate of single valve at 30 degrees with 3 inlets

One valve with three inlets under Laminar model	Name	Mass Flow Rate	Absolute
	QInlet-1	0.29400006	0.29400006
	QInlet-2	0.085750043	0.085750043
	QInlet-3	0.36750001	0.36750001
	QOutlet-1	-0.34324962	0.34324962
	QOutlet-2	-0.29972315	0.29972315
	QOutlet-3	-0.10427718	0.10427718
	QInlet-total	0.747250113	0.747250113
	Qoutlet-total	-0.74724995	0.74724995
	Mass conversion	Qin - Qout	1.63E-07
	Percentage go into valve	$(Out2+Out3-In3)/(In1+In2)$	9.611668229
	Percentage not go into valve	$(Out1)/(In1+In2)$	90.38828885
	Total	99.99995708	

Table 4.7 Mass flow rate of single valve at 15 degrees with 3 inlets

One valve with three inlets under Laminar model	Name	Mass Flow Rate	Absolute
	QInlet-1	0.29400006	0.29400006
	QInlet-2	0.085750043	0.085750043
	QInlet-3	0.36750007	0.36750007
	QOutlet-1	-0.35662535	0.35662535
	QOutlet-2	-0.38305256	0.38305256
	QOutlet-3	-0.007671785	0.007671785
	QInlet-total	0.747250173	0.747250173
	Qoutlet-total	-0.747349695	0.747349695
	Mass conversion	Qin - Qout	-9.9522E-05
	Percentage go into valve	$(Out2+Out3-In3)/(In1+In2)$	6.115673154
	Percentage not go into valve	$(Out1)/(In1+In2)$	93.91053411
	Total	100.0262073	

Table 4.8 Mass flow rate of single valve at 3 degrees with 3 inlets

	Name	Mass Flow Rate	Absolute	
One valve with three inlets under Laminar model	QInlet-1	0.29400006	0.29400006	
	QInlet-2	0.085750043	0.085750043	
	QInlet-3	0.37134558	0.37134558	
	QOutlet-1	-0.37622598	0.37622598	
	QOutlet-2	-0.36817992	0.36817992	
	QOutlet-3	-0.006673151	0.006673151	
	QInlet-total	0.751095683	0.751095683	
	Qoutlet-total	-0.751079051	0.751079051	
	Mass conversion	Qin - Qout		1.66323E-05
	Percentage go into valve	$(\text{Out2}+\text{Out3}-\text{In3})/(\text{In1}+\text{In2})$		0.92363127
	Percentage not go into valve	$(\text{Out1})/(\text{In1}+\text{In2})$		99.07198893
		Total		99.9956202

4.1.1.2 Single valve with Transition SST model

This part shows the mass flow rate and percentage of air going through the valve from 45 degrees to 3 degrees of type 1 and type 2 transition SST model. It can be seen the greater the angle of the valve, the greater the percentage of air goes through the valve when there are only two inlets from table 4.9 to 4.16.

Table 4.9 Mass flow rate of single valve at 45 degrees with 2 inlets

One valve with two inlets under SST viscous model	Name	Mass Flow Rate	Absolute
	QInlet-1	0.29400006	0.29400006
	QInlet-2	0.085749969	0.085749969
	QOutlet-1	-0.33179864	0.33179864
	QOutlet-2	-0.070796877	0.070796877
	QOutlet-3	0.022845048	0.022845048
	QInlet-total	0.379750029	0.379750029
	Qoutlet-total	-0.379750469	0.379750469
	Mass conversion	Qin - Qout	5.7742E-08
	Percentage go into valve	$(\text{Out2}+\text{out3})/(\text{In1}+\text{In2})$	12.58637745
	Percentage not go into valve	$(\text{Out1})/(\text{In1}+\text{In2})$	87.41360754
		Total	99.99998499

Table 4.10 Mass flow rate of single valve at 30 degrees with 2 inlets

One valve with two inlets under SST viscous model	Name	Mass Flow Rate	Absolute
	QInlet-1	0.29400006	0.29400006
	QInlet-2	0.085750043	0.085750043
	QOutlet-1	-0.33821702	0.33821702
	QOutlet-2	-0.055714697	0.055714697
	QOutlet-3	0.014181707	0.014181707
	QInlet-total	0.379750103	0.379750103
	Qoutlet-total	-0.37975001	0.37975001
	Mass conversion	Qin - Qout	9.3E-08
	Percentage go into valve	$(\text{Out2}+\text{out3})/(\text{In1}+\text{In2})$	10.93692659
	Percentage not go into valve	$(\text{Out1})/(\text{In1}+\text{In2})$	89.06304892
		Total	99.99997551

Table 4.11 Mass flow rate of single valve at 15 degrees with 2 inlets

One valve with two inlets under SST viscous model	Name	Mass Flow Rate	Absolute
	QInlet-1	0.29400006	0.29400006
	QInlet-2	0.085750043	0.085750043
	QOutlet-1	-0.35575268	0.35575268
	QOutlet-2	-0.035454798	0.035454798
	QOutlet-3	0.011457537	0.011457537
	QInlet-total	0.379750103	0.379750103
	Qoutlet-total	-0.379749941	0.379749941
	Mass conversion	Qin - Qout	1.62E-07
	Percentage go into valve	(Out2+out3)/(In1+In2)	6.319224356
	Percentage not go into valve	(Out1)/(In1+In2)	93.68073298
		Total	99.99995734

Table 4.12 Mass flow rate of single valve at 3 degrees with 2 inlets

One valve with two inlets under SST viscous model	Name	Mass Flow Rate	Absolute
	QInlet-1	0.29400003	0.29400003
	QInlet-2	0.085750043	0.085750043
	QOutlet-1	-0.37625816	0.37625816
	QOutlet-2	-0.007934903	0.007934903
	QOutlet-3	0.004442982	0.004442982
	QInlet-total	0.379750073	0.379750073
	Qoutlet-total	-0.37975008	0.37975008
	Mass conversion	Qin - Qout	-7.4E-09
	Percentage go into valve	(Out2+out3)/(In1+In2)	0.919531199
	Percentage not go into valve	(Out1)/(In1+In2)	99.08047075
		Total	100.0000019

Table 4.13 Mass flow rate of single valve at 45 degrees with 3 inlets

	Name	Mass Flow Rate	Absolute
One valve with three inlets under SST viscous model	QInlet-1	0.29400003	0.29400003
	QInlet-2	0.085750051	0.085750051
	QInlet-3	0.36750001	0.36750001
	QOutlet-1	-0.33711681	0.33711681
	QOutlet-2	-0.33689833	0.33689833
	QOutlet-3	-0.073235333	0.073235333
	QInlet-total	0.747250091	0.747250091
	Qoutlet-total	-0.747250473	0.747250473
	Mass conversion	Qin - Qout	7.4506E-08
	Percentage go into valve	$(\text{Out2}+\text{Out3}-\text{In3})/(\text{In1}+\text{In2})$	11.22676601
	Percentage not go into valve	$(\text{Out1})/(\text{In1}+\text{In2})$	88.77333459
		Total	100.0001006

Table 4.14 Mass flow rate of single valve at 30 degrees with 3 inlets

	Name	Mass Flow Rate	Absolute
One valve with three inlets under SST viscous model	QInlet-1	0.29400006	0.29400006
	QInlet-2	0.085750043	0.085750043
	QInlet-3	0.36750001	0.36750001
	QOutlet-1	-0.33827323	0.33827323
	QOutlet-2	-0.35890588	0.35890588
	QOutlet-3	-0.050070912	0.050070912
	QInlet-total	0.747250113	0.747250113
	Qoutlet-total	-0.747250022	0.747250022
	Mass conversion	Qin - Qout	9.1E-08
	Percentage go into valve	$(\text{Out2}+\text{Out3}-\text{In3})/(\text{In1}+\text{In2})$	10.92212528
	Percentage not go into valve	$(\text{Out1})/(\text{In1}+\text{In2})$	89.07785076
		Total	99.99995708

Table 4.15 Mass flow rate of single valve at 15 degrees with 3 inlets

	Name	Mass Flow Rate	Absolute
One valve with three inlets under SST viscous model	QInlet-1	0.29400006	0.29400006
	QInlet-2	0.085750043	0.085750043
	QInlet-3	0.36750007	0.36750007
	QOutlet-1	-0.3550171	0.3550171
	QOutlet-2	-0.38445556	0.38445556
	QOutlet-3	-0.007777439	0.007777439
	QInlet-total	0.747250173	0.747250173
	Qoutlet-total	-0.747250099	0.747250099
	Mass conversion	Qin - Qout	7.45E-08
	Percentage go into valve	$(Out2+Out3-In3)/(In1+In2)$	6.512948464
	Percentage not go into valve	$(Out1)/(In1+In2)$	93.48703192
	Total	99.99998038	

Table 4.16 Mass flow rate of single valve at 3 degrees with 3 inlets

	Name	Mass Flow Rate	Absolute
One valve with three inlets under SST viscous model	QInlet-1	0.29400006	0.29400006
	QInlet-2	0.085750043	0.085750043
	QInlet-3	0.37134558	0.37134558
	QOutlet-1	-0.37627327	0.37627327
	QOutlet-2	-0.37168619	0.37168619
	QOutlet-3	-0.003136295	0.003136295
	QInlet-total	0.751095683	0.751095683
	Qoutlet-total	-0.751095755	0.751095755
	Mass conversion	Qin - Qout	-7.21E-08
	Percentage go into valve	$(Out2+Out3-In3)/(In1+In2)$	0.915577132
	Percentage not go into valve	$(Out1)/(In1+In2)$	99.08444185
	Total	100.000019	

4.1.1.3 Double valves with laminar model

This part shows the mass flow rate and percentage of air going through the valve from 45 degrees to 3 degrees of type 3 and type 4 laminar model. The percentage of air go through two valves is nearly double that of the single valve.

Table 4.17 Mass flow rate of double valves at 45 degrees with 2 inlets

	Name	Mass Flow Rate	Absolute	
Two valves with two inlets under laminar viscous mode	QInlet-1	0.22050211	0.22050211	
	QInlet-2	0.050225005	0.050225005	
	QOutlet-1	-0.21336778	0.21336778	
	QOutlet-2	-0.059796531	0.059796531	
	QOutlet-3	0.002437165	0.002437165	
	QInlet-total	0.270727115	0.270727115	
	Qoutlet-total	-0.270727146	0.270727146	
	Mass conversion	Qin - Qout		-2.794E-08
	Percentage go into valve	(Out2+out3)/(In1+In2)		21.18715224
	Percentage not go into valve	(Out1)/(In1+In2)		78.81285921
		Total		100.0000115

Table 4.18 Mass flow rate of double valves at 30 degrees with 2 inlets

	Name	Mass Flow Rate	Absolute	
Two valves with two inlets under laminar viscous mode	QInlet-1	0.22050214	0.22050214	
	QInlet-2	0.050225019	0.050225019	
	QOutlet-1	-0.21485442	0.21485442	
	QOutlet-2	-0.057921667	0.057921667	
	QOutlet-3	0.00204896	0.00204896	
	QInlet-total	0.270727159	0.270727159	
	Qoutlet-total	-0.270727127	0.270727127	
	Mass conversion	Qin - Qout		3.24E-08
	Percentage go into valve	(Out2+out3)/(In1+In2)		20.63801312
	Percentage not go into valve	(Out1)/(In1+In2)		79.36197491
		Total		99.99998803

Table 4.19 Mass flow rate of double valves at 15 degrees with 2 inlets

Two valves with two inlets under laminar viscous mode	Name	Mass Flow Rate	Absolute
	QInlet-1	0.22050199	0.22050199
	QInlet-2	0.050225005	0.050225005
	QOutlet-1	-0.22937392	0.22937392
	QOutlet-2	-0.043456018	0.043456018
	QOutlet-3	0.002102808	0.002102808
	QInlet-total	0.270726995	0.270726995
	Qoutlet-total	-0.27072713	0.27072713
	Mass conversion	Qin - Qout	-1.354E-07
	Percentage go into valve	$(\text{Out2}+\text{out3})/(\text{In1}+\text{In2})$	15.27487512
	Percentage not go into valve	$(\text{Out1})/(\text{In1}+\text{In2})$	84.72517489
		Total	100.00005

Table 4.20 Mass flow rate of double valves at 3 degrees with 2 inlets

Two valves with two inlets under laminar viscous mode	Name	Mass Flow Rate	Absolute
	QInlet-1	0.22050247	0.22050247
	QInlet-2	0.050225087	0.050225087
	QOutlet-1	-0.26209533	0.26209533
	QOutlet-2	-0.009479294	0.009479294
	QOutlet-3	0.000847503	0.000847503
	QInlet-total	0.270727557	0.270727557
	Qoutlet-total	-0.270727121	0.270727121
	Mass conversion	Qin - Qout	4.3636E-07
	Percentage go into valve	$(\text{Out2}+\text{out3})/(\text{In1}+\text{In2})$	3.188367943
	Percentage not go into valve	$(\text{Out1})/(\text{In1}+\text{In2})$	96.81147088
		Total	99.99983882

Table 4.21 Mass flow rate of double valves at 45 degrees with 3 inlets

Two valves with three inlets under Laminar model	Name	Mass Flow Rate	Absolute
	QInlet-1	0.22050217	0.22050217
	QInlet-2	0.050224956	0.050224956
	QInlet-3	0.27247247	0.27247247
	QOutlet-1	-0.20410982	0.20410982
	QOutlet-2	-0.26448604	0.26448604
	QOutlet-3	-0.074603558	0.074603558
	QInlet-total	0.543199596	0.543199596
	Qoutlet-total	-0.543199418	0.543199418
	Mass conversion	Qin - Qout	1.7509E-07
	Percentage go into valve	(Out2+out3)/(In1+In2)	24.60674295
	Percentage not go into valve	(Out1)/(In1+In2)	75.3931913
	Total	99.99993425	

Table 4.22 Mass flow rate of double valves at 30 degrees with 3 inlets

Two valves with three inlets under Laminar model	Name	Mass Flow Rate	Absolute
	QInlet-1	0.22050214	0.22050214
	QInlet-2	0.050225019	0.050225019
	QInlet-3	0.25724986	0.25724986
	QOutlet-1	-0.21089971	0.21089971
	QOutlet-2	-0.2575371	0.2575371
	QOutlet-3	-0.059540298	0.059540298
	QInlet-total	0.527977019	0.527977019
	Qoutlet-total	-0.527977108	0.527977108
	Mass conversion	Qin - Qout	-8.9E-08
	Percentage go into valve	(Out2+out3)/(In1+In2)	22.09883124
	Percentage not go into valve	(Out1)/(In1+In2)	77.90120163
	Total	100.0000329	

Table 4.23 Mass flow rate of double valves at 15 degrees with 3 inlets

Two valves with three inlets under Laminar model	Name	Mass Flow Rate	Absolute
	QInlet-1	0.22050199	0.22050199
	QInlet-2	0.050225005	0.050225005
	QInlet-3	0.23952308	0.23952308
	QOutlet-1	-0.23101489	0.23101489
	QOutlet-2	-0.24676721	0.24676721
	QOutlet-3	-0.032468192	0.032468192
	QInlet-total	0.510250075	0.510250075
	Qoutlet-total	-0.510250292	0.510250292
	Mass conversion	Qin - Qout	-2.17E-07
	Percentage go into valve	$(\text{Out2}+\text{out3})/(\text{In1}+\text{In2})$	14.66877066
	Percentage not go into valve	$(\text{Out1})/(\text{In1}+\text{In2})$	85.3313095
		Total	100.0000802

Table 4.24 Mass flow rate of double valves at 3 degrees with 2 inlets

Two valves with three inlets under Laminar model	Name	Mass Flow Rate	Absolute
	QInlet-1	0.22050247	0.22050247
	QInlet-2	0.050225087	0.050225087
	QInlet-3	0.22434606	0.22434606
	QOutlet-1	-0.26205039	0.26205039
	QOutlet-2	-0.22737448	0.22737448
	QOutlet-3	-0.005736291	0.005736291
	QInlet-total	0.495073617	0.495073617
	Qoutlet-total	-0.495161161	0.495161161
	Mass conversion	Qin - Qout	-8.754E-05
	Percentage go into valve	$(\text{Out2}+\text{out3})/(\text{In1}+\text{In2})$	3.237465553
	Percentage not go into valve	$(\text{Out1})/(\text{In1}+\text{In2})$	96.79487116
		Total	100.0323367

4.1.1.4 Double valves with Transition SST model

This part shows the mass flow rate and percentage of air going through valve from 45 degrees to 3 degrees of type 3 and type 4 laminar model.

Table 4.25 Mass flow rate of double valves at 45 degrees with 2 inlets

Two valves with two inlets under SST viscous model	Name	Mass Flow Rate	Absolute
	QInlet-1	0.22050217	0.22050217
	QInlet-2	0.050224956	0.050224956
	QOutlet-1	-0.21188101	0.21188101
	QOutlet-2	-0.068216704	0.068216704
	QOutlet-3	0.009370515	0.009370515
	QInlet-total	0.270727126	0.270727126
	Qoutlet-total	-0.270727199	0.270727199
	Mass conversion	Qin - Qout	-7.6368E-08
	Percentage go into valve	$(\text{Out2}+\text{out3})/(\text{In1}+\text{In2})$	21.73634751
	Percentage not go into valve	$(\text{Out1})/(\text{In1}+\text{In2})$	78.26367942
		Total	100.0000269

Table 4.26 Mass flow rate of double valves at 30 degrees with 2 inlets

Two valves with two inlets under SST viscous model	Name	Mass Flow Rate	Absolute
	QInlet-1	0.22050214	0.22050214
	QInlet-2	0.050225019	0.050225019
	QOutlet-1	-0.20547977	0.20547977
	QOutlet-2	-0.072532646	0.072532646
	QOutlet-3	0.007285453	0.007285453
	QInlet-total	0.270727159	0.270727159
	Qoutlet-total	-0.270726963	0.270726963
	Mass conversion	Qin - Qout	1.964E-07
	Percentage go into valve	$(\text{Out2}+\text{out3})/(\text{In1}+\text{In2})$	24.10071928
	Percentage not go into valve	$(\text{Out1})/(\text{In1}+\text{In2})$	75.89920818
		Total	99.99992745

Table 4.27 Mass flow rate of double valves at 15 degrees with 2 inlets

Two valves with two inlets under SST viscous model	Name	Mass Flow Rate	Absolute
	QInlet-1	0.22050199	0.22050199
	QInlet-2	0.050225005	0.050225005
	QOutlet-1	-0.22885604	0.22885604
	QOutlet-2	-0.046426062	0.046426062
	QOutlet-3	0.004554954	0.004554954
	QInlet-total	0.270726995	0.270726995
	Qoutlet-total	-0.270727148	0.270727148
	Mass conversion	Qin - Qout	-1.526E-07
	Percentage go into valve	$(\text{Out2}+\text{out3})/(\text{In1}+\text{In2})$	15.46617381
	Percentage not go into valve	$(\text{Out1})/(\text{In1}+\text{In2})$	84.53388256
		Total	100.0000564

Table 4.28 Mass flow rate of double valves at 3 degrees with 2 inlets

Two valves with two inlets under SST viscous model	Name	Mass Flow Rate	Absolute
	QInlet-1	0.22050247	0.22050247
	QInlet-2	0.050224997	0.050224997
	QOutlet-1	-0.26217651	0.26217651
	QOutlet-2	-0.011631961	0.011631961
	QOutlet-3	0.003081536	0.003081536
	QInlet-total	0.270727467	0.270727467
	Qoutlet-total	-0.270726935	0.270726935
	Mass conversion	Qin - Qout	5.319E-07
	Percentage go into valve	$(\text{Out2}+\text{out3})/(\text{In1}+\text{In2})$	3.158314594
	Percentage not go into valve	$(\text{Out1})/(\text{In1}+\text{In2})$	96.84148894
	Total	99.99980353	

Table 4.29 Mass flow rate of double valves at 45 degrees with 3 inlets

Two valves with three inlets under SST viscous model	Name	Mass Flow Rate	Absolute
	QInlet-1	0.22050217	0.22050217
	QInlet-2	0.050224956	0.050224956
	QInlet-3	0.27247247	0.27247247
	QOutlet-1	-0.20282407	0.20282407
	QOutlet-2	-0.25414976	0.25414976
	QOutlet-3	-0.086225681	0.086225681
	QInlet-total	0.543199596	0.543199596
	Qoutlet-total	-0.543199511	0.543199511
	Mass conversion	Qin - Qout	1.7509E-07
	Percentage go into valve	(Out2+out3)/(In1+In2)	24.60674295
	Percentage not go into valve	(Out1)/(In1+In2)	75.3931913
		Total	99.9999342

Table 4.30 Mass flow rate of double valves at 30 degrees with 3 inlets

Two valves with three inlets under SST viscous model	Name	Mass Flow Rate	Absolute
	QInlet-1	0.22050214	0.22050214
	QInlet-2	0.050225019	0.050225019
	QInlet-3	0.25724986	0.25724986
	QOutlet-1	-0.20733091	0.20733091
	QOutlet-2	-0.25462142	0.25462142
	QOutlet-3	-0.066024825	0.066024825
	QInlet-total	0.527977019	0.527977019
	Qoutlet-total	-0.527977155	0.527977155
	Mass conversion	Qin - Qout	-1.36E-07
	Percentage go into valve	(Out2+out3)/(In1+In2)	23.41707616
	Percentage not go into valve	(Out1)/(In1+In2)	76.58297408
		Total	100.0000502

Table 4.31 Mass flow rate of double valves at 15 degrees with 3 inlets

Two valves with three inlets under SST viscous model	Name	Mass Flow Rate	Absolute
	QInlet-1	0.22050199	0.22050199
	QInlet-2	0.050225005	0.050225005
	QInlet-3	0.23952308	0.23952308
	QOutlet-1	-0.23002109	0.23002109
	QOutlet-2	-0.25054899	0.25054899
	QOutlet-3	-0.029680211	0.029680211
	QInlet-total	0.510250075	0.510250075
	Qoutlet-total	-0.510250291	0.510250291
	Mass conversion	Qin - Qout	-2.16E-07
	Percentage go into valve	$(\text{Out2}+\text{out3})/(\text{In1}+\text{In2})$	15.03585596
	Percentage not go into valve	$(\text{Out1})/(\text{In1}+\text{In2})$	84.96422383
	Total	100.0000798	

Table 4.32 Mass flow rate of double valves at 45 degrees with 3 inlets

Two valves with three inlets under SST viscous model	Name	Mass Flow Rate	Absolute
	QInlet-1	0.22050247	0.22050247
	QInlet-2	0.050225087	0.050225087
	QInlet-3	0.22434606	0.22434606
	QOutlet-1	-0.26212195	0.26212195
	QOutlet-2	-0.22701854	0.22701854
	QOutlet-3	-0.005933398	0.005933398
	QInlet-total	0.495073617	0.495073617
	Qoutlet-total	-0.495073888	0.495073888
	Mass conversion	Qin - Qout	-2.709E-07
	Percentage go into valve	$(\text{Out2}+\text{out3})/(\text{In1}+\text{In2})$	3.178796424
	Percentage not go into valve	$(\text{Out1})/(\text{In1}+\text{In2})$	96.82130364
	Total	100.0001001	

4.1.2 Velocity streamline

This part shows the velocity streamline of single valve and two valves model in the simulation. When the valve degree is small, the velocity of air through the valve is very small and the degree is small as well. The greater the angle of the one way valve, the faster the airflow through the valve and the degree of the air is greater. Some vortex can be observed on two valves model at 45 degrees. Figure 4.5 to figure 4.8 shows the velocity of valves at different angles.

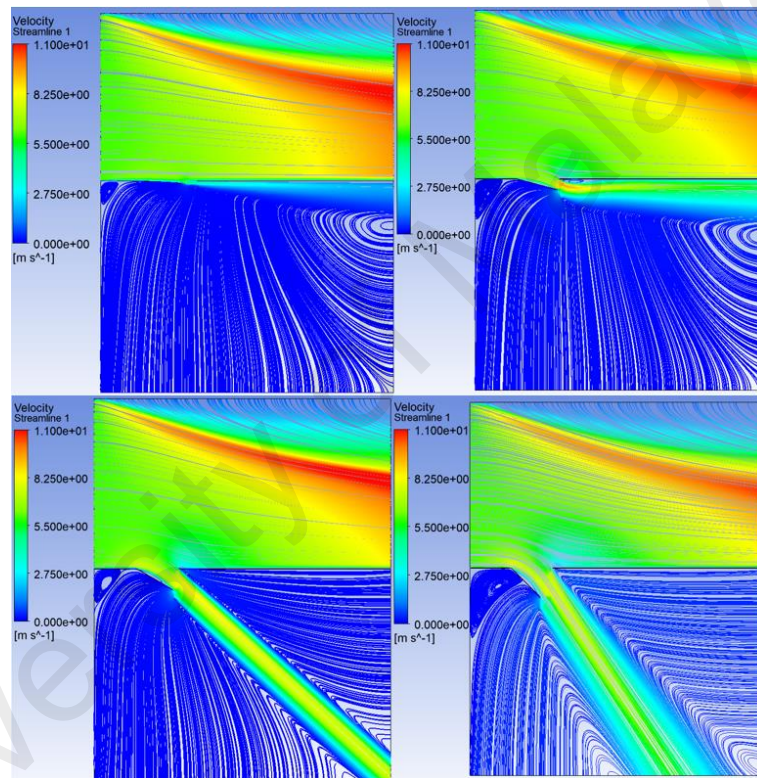


Figure 4.5 Velocity streamline of one valve mechanism at 4 types of degree with two inlets

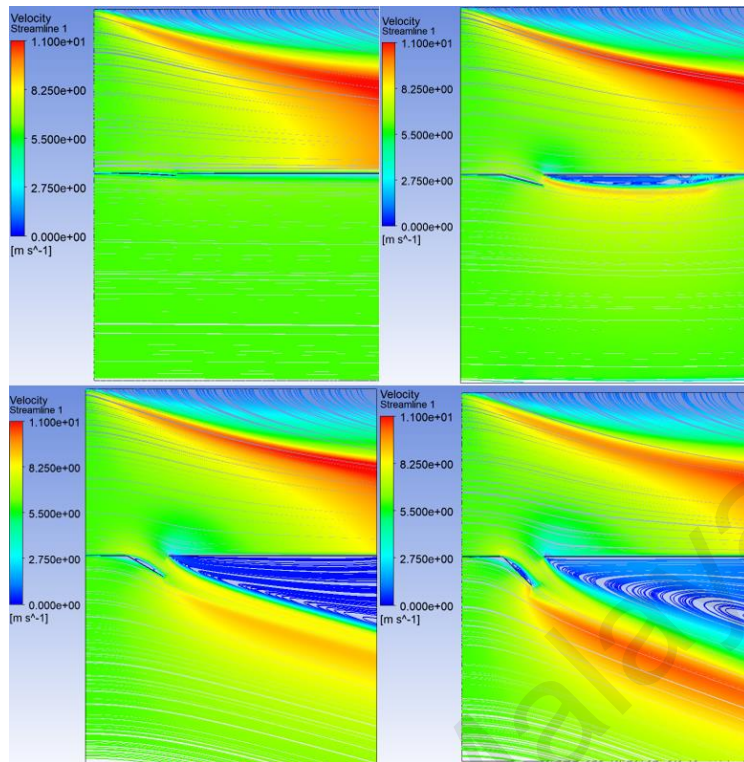


Figure 4.6 Velocity streamline of one valve mechanism at 4 types of degree with three inlets

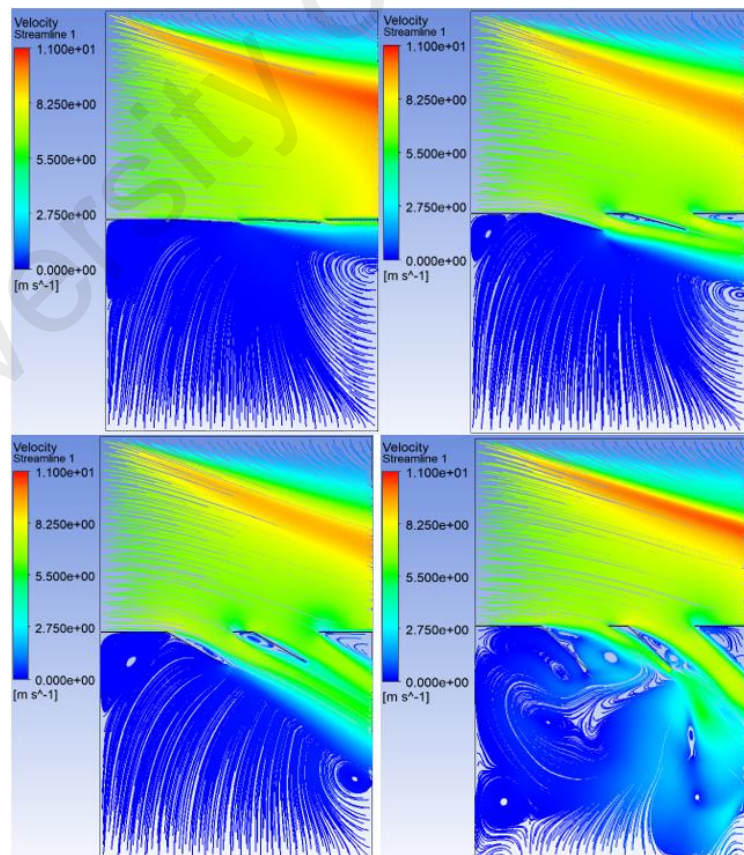


Figure 4.7 Velocity streamline of two valves mechanism at 4 types of degree with two inlets

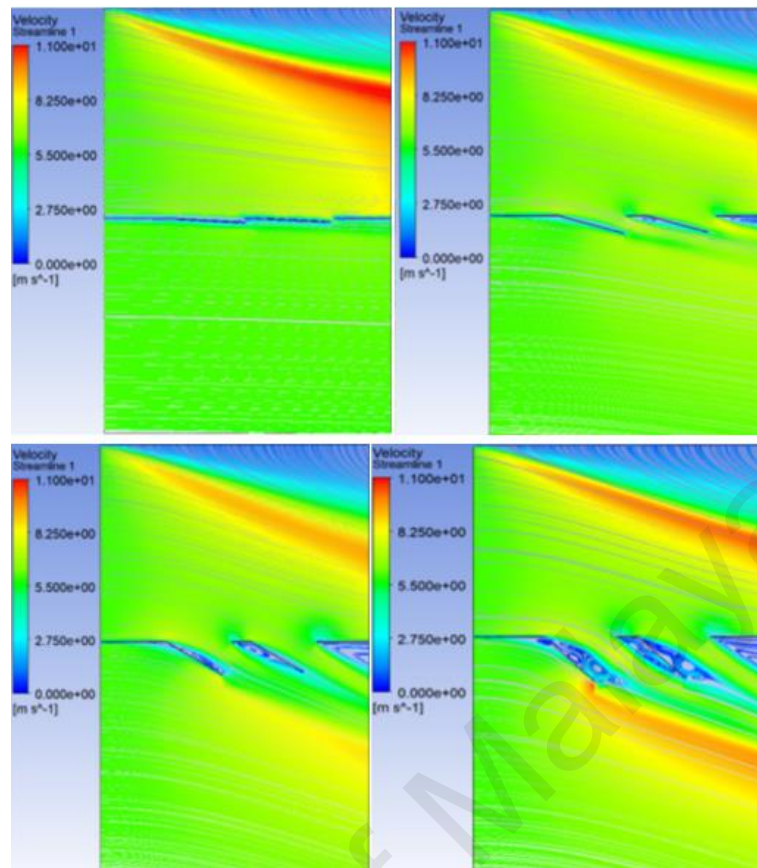


Figure 4.8 Velocity streamline of two valves mechanism at 4 types of degree with three inlets

4.1.3 Pressure

This part shows the distribution of pressure on valves and part of the wing. It is observed that the pressure on the upper surface of one way valves gets smaller when the valve opens larger, and the pressure on the lower surface gets larger. That means it can get a larger lift force and less drag force. This phenomenon is more obvious in the two valves model. Figure 4.9 to figure 4.12 shows the pressure contour of the models at different angles of valves.

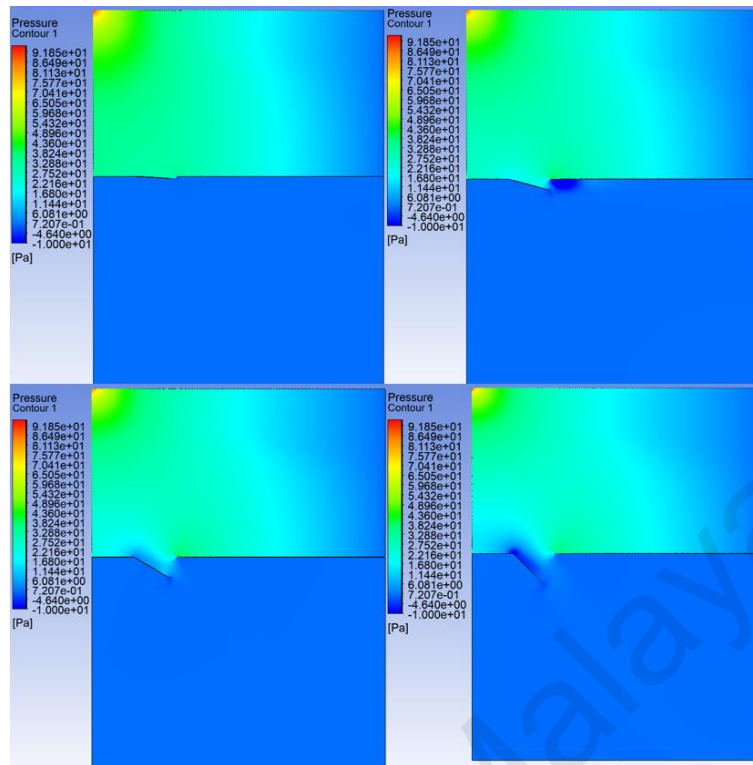


Figure 4.9 Pressure contour of one valve mechanism at 4 types of degree with two inlets

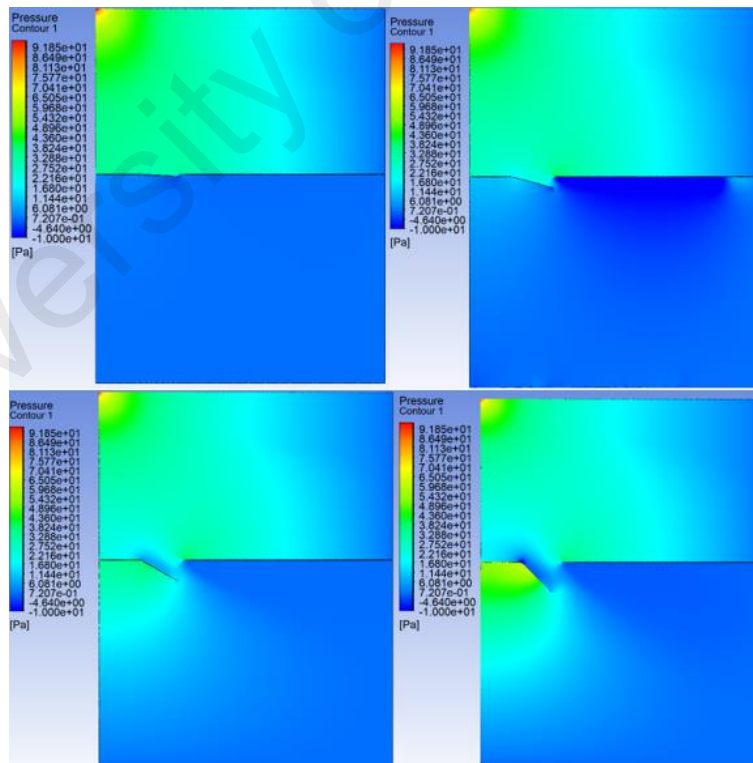


Figure 4.10 Pressure contour of one valve mechanism at 4 types of degree with three inlets

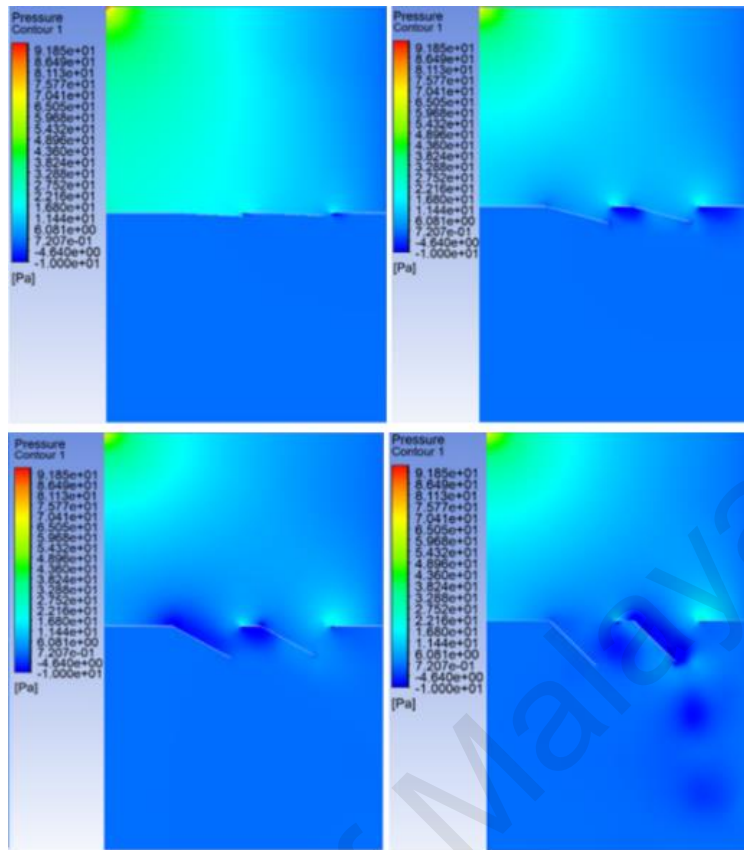


Figure 4.11 Pressure contour of two valves mechanism at 4 types of degree with two inlets

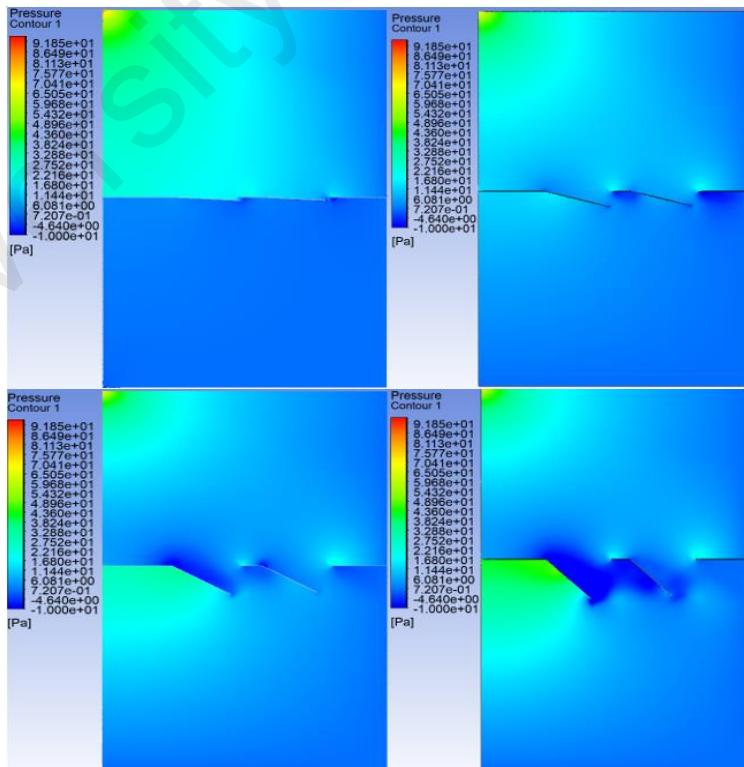


Figure 4.12 Pressure contour of two valves mechanism at 4 types of degree with three inlets

4.1.4 Lift and drag

As an important parameter to verify flight capability, the detailed value of drag force, lift force, CD and CF are showed from table 4.33 to 4.40. Each table represents a one way valve angle from 45 degrees to 3 degrees. The model type referred to figure 4.1 to figure 4.4.

Table 4.33 Drag force and CD for different type valves at 45 degrees valve angle

Number of valves	Type	Drag Force Total	Drag Force Coefficient
Two valves	T4-SST	0.4093939	0.6683982
	T4-Laminar	0.40938259	0.66837974
	T3-SST	0.14041267	0.22924518
	T3-Laminar	0.12315457	0.20841563
Single valve	T2-SST	0.14022756	0.22894296
	T2-Laminar	0.14622111	0.23872835
	T1-SST	0.048745503	0.083053882
	T1-Laminar	0.053815765	0.087862474

Table 4.34 Drag force and CD for different type valves at 30 degrees valve angle

Number of valves	Type	Drag Force Total	Drag Force Coefficient
Two valves	T4-SST	0.19943858	0.3256140
	T4-Laminar	0.17810939	0.29446431
	T3-SST	0.05512889	0.09000636
	T3-Laminar	0.05646215	0.09218310
Single valve	T2-SST	0.11871232	0.19381603
	T2-Laminar	0.12114372	0.21043873
	T1-SST	0.00282736	0.00461610
	T1-Laminar	0.00254311	0.00428671

Table 4.35 Drag force and CD for different type valves at 15 degrees valve angle

Number of valves	Type	Drag Force Total	Drag Force Coefficient
Two valves	T4-SST	0.045456793	0.07611313
	T4-Laminar	0.044172698	0.07211869
	T3-SST	0.004198206	0.00811952
	T3-Laminar	0.003992191	0.00651786
Single valve	T2-SST	0.007285577	0.01438462
	T2-Laminar	0.006933643	0.01132023
	T1-SST	0.001491934	0.00243581
	T1-Laminar	0.000920224	0.00191873

Table 4.36 Drag force and CD for different type valves at 3 degrees valve angle

Number of valves	Type	Drag Force Total	Drag Force Coefficient
Two valves	T4-SST	0.03607443	0.05889703
	T4-Laminar	0.035043227	0.05721343
	T3-SST	0.026579916	0.04339578
	T3-Laminar	0.025728742	0.04200611
Single valve	T2-SST	0.043993081	0.07182544
	T2-Laminar	0.040917382	0.06680389
	T1-SST	0.033622085	0.0548932
	T1-Laminar	0.03215841	0.05250353

Table 4.37 Lift force and CF for different type valves at 45 degrees valve angle

Number of valves	Type	Lift Force Total	Lift Force Coefficient
Two valves	T4-SST	0.74365153	1.214125
	T4-Laminar	0.74360388	1.2140472
	T3-SST	-0.07277599	-0.12085877
	T3-Laminar	-0.08321845	-0.13586685
Single valve	T2-SST	-0.73769796	-1.2044048
	T2-Laminar	-0.65136854	-1.0675405
	T1-SST	-1.0712194	-1.6917867
	T1-Laminar	-0.94267893	-1.5390676

Table 4.38 Lift force and CF for different type valves at 30 degrees valve angle

Number of valves	Type	Lift Force Total	Lift Force Coefficient
Two valves	T4-SST	0.44537855	0.72714865
	T4-Laminar	0.41501932	0.67962338
	T3-SST	-0.10869221	-0.17480361
	T3-Laminar	-0.1250915	-0.20423102
Single valve	T2-SST	-1.0081008	-1.6458788
	T2-Laminar	-1.0423193	-1.8854192
	T1-SST	-1.286111	-1.8834465
	T1-Laminar	-1.099889	-1.7957359

Table 4.39 Lift force and CF for different type valves at 15 degrees valve angle

Number of valves	Type	Lift Force Total	Lift Force Coefficient
Two valves	T4-SST	-0.11469346	-0.17358116
	T4-Laminar	-0.09098695	-0.14855013
	T3-SST	-0.35952189	-0.58697452
	T3-Laminar	-0.34424978	-0.56204046
Single valve	T2-SST	-1.5387969	-2.4857909
	T2-Laminar	-1.5503805	-2.5312335
	T1-SST	-1.3670121	-2.2318565
	T1-Laminar	-1.4198485	-2.31812

Table 4.40 Lift force and CF for different type valves at 3 degrees valve angle

Number of valves	Type	Lift Force Total	Lift Force Coefficient
Two valves	T4-SST	-0.55405352	-0.9046
	T4-Laminar	-0.56149601	-0.9167
	T3-SST	-0.59352847	-0.969
	T3-Laminar	-0.60851708	-0.9935
Single valve	T2-SST	-1.4819279	-2.4195
	T2-Laminar	-1.5116249	-2.468
	T1-SST	-1.4982594	-2.4461
	T1-Laminar	-1.5231905	-2.4868

By comparing table 4.33 to table 4.36, it can be easily observed that the drag force and CD increase with the opening angle of the one way valve because the increasing of the

contact area of the valve and the airflow, while the lift force also increases with the increasing of valve angle. The difference between the laminar model and the transition SST model is only 5% to 10%. The drag force increases more than 50% when there is one more inlet below the wing except for 3 degrees. In addition, the drag force and lift force of two valves are bigger than single valve when the angle of the valve larger than 3 degrees. The percentage of increase is around 50%.

4.2 Experimental

4.2.1 Actual model

The one way valve mechanism designed based on ANSYS analysis is installed on the wings in the real experiment. There are three types of wings designed for the test. The first type has only one row of valves in the front section of the wing. The dimension of the wing part is showed in Appendix B (type 1 wing). The second type has the same position of the one way valve but the valve direction is backward which is shown in Appendix B (type 2 wing). The last type of wing has valves covered the entire wing area which is shown in Appendix B (type 3 wing).

4.2.2 Testing flight performance

This research tested the flight performance of four types of wings including wing without one way valve, type 1 wing, type 2 wing and type 3 wing. The test site was operated outdoor. The testing utilized the model with a 20-degree tail to ensure the minimum impact from the body. In the comparison of duration of the flight, the type 3 wing got the best result and the duration of the type 2 wing is smaller than no valve wing. The first type of wing is almost unable to fly due to the excessive number of valves that destroys the function of the wing. It can only fly 20 seconds before falling to the ground and it has a chaotic flight path. The second type of wing has valves with forwarding direction. Therefore, the direction of air flowing through the valve conflicts with the flight

direction of the flapping drone which generates more drag force. At the same time, the second type cannot be controlled very well compared with no valve wing. During the flight, the lift and landing could be adjusted by controlling the flight speed. The hovering can also be controlled by the magnetic actuator on the tail. The third type of wing got the best performance during this test. It has the longest duration of the flight; the highest altitude and its control of flight is also better than the wing without valve. The flight performance test is consistent with CFD simulation. Table 4.37 shows the details of the testing results. Figure 4.13 and figure 4.14 briefly shows the actual flight test.

Table 4.41 Testing results of four types of wings

Angle of tail	Type of wing	Duration of flight	Maximum flight altitude	Flight Stability
20	No valve	411s	6.35m	7/10
20	Type 1	20s	1.5m	1/10
20	Type 2	327s	5.5m	6/10
20	Type 3	434s	9m	9/10



Figure 4.13 Actual flight of testing I



Figure 4.14 Actual flight of testing II

4.2.3 Velocity profile

To investigate the lift of the wing by the check valve in more detail, the velocity generated by wings need to be measured. In this velocity test type 2 and type 3 wings were tested. The first type of wing was eliminated because it failed the flight performance test. The measurement method has been explained in Chapter 3. Plane 4 is not included in the test because the velocity measured at that plane is zero. Since the power supply of the drone during the test is provided by the battery, the flapping frequency was set to the lowest to ensure the efficiency and stability of the test. The table of velocity data collected through the experiment is shown in Appendix C. Figure 4.14 to figure 4.18 shows the velocity profile for three types of wings.

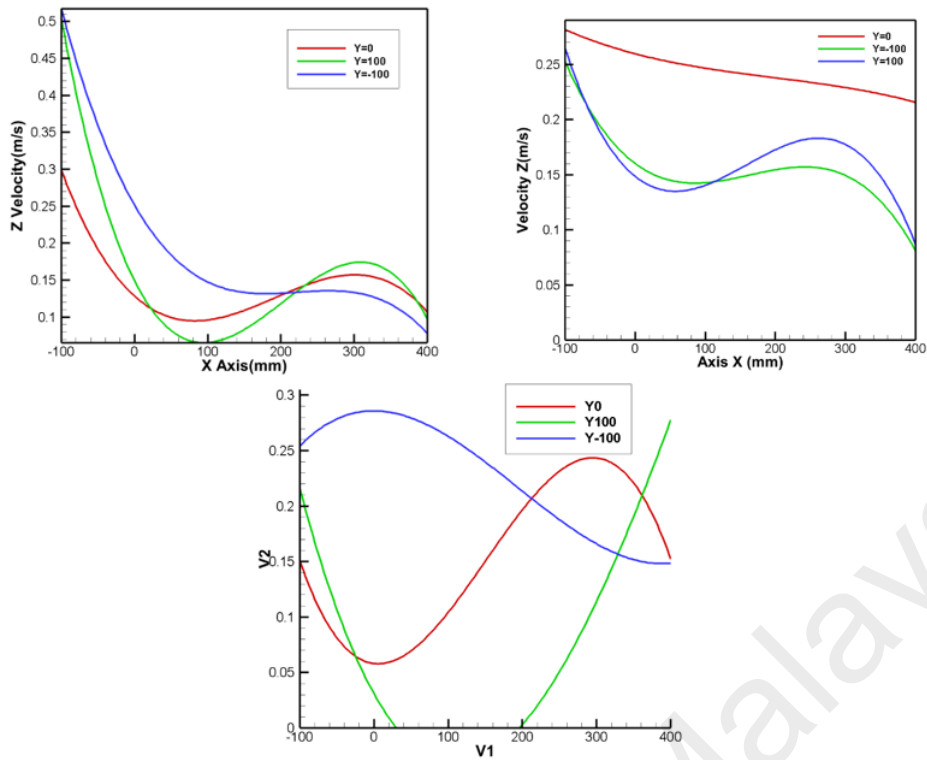


Figure 4.15 Velocity Z at Z=100mm. Type 2 wing (Left) non-valve wing (Right) and type 3 wing (Below)

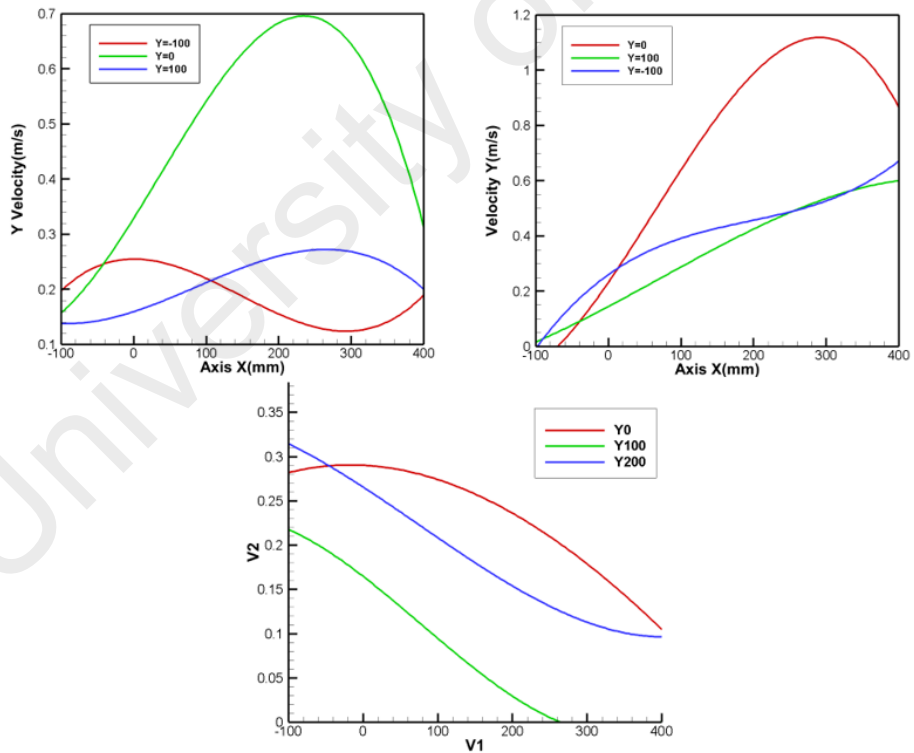


Figure 4.16 Velocity Y at Z=100mm. Type 2 wing (Left) non-valve wing (Right) and type 3 wing (Below)

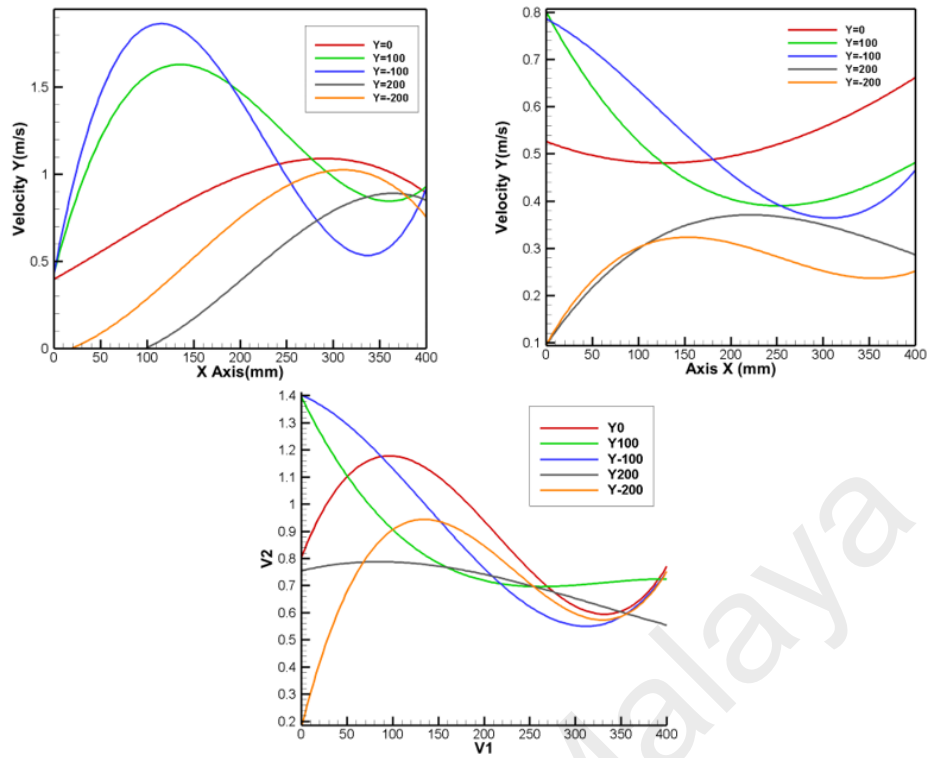


Figure 4.17 Velocity Y at Z=0. Type 2 wing (Left) non-valve wing (Right) and type 3 wing (Below)

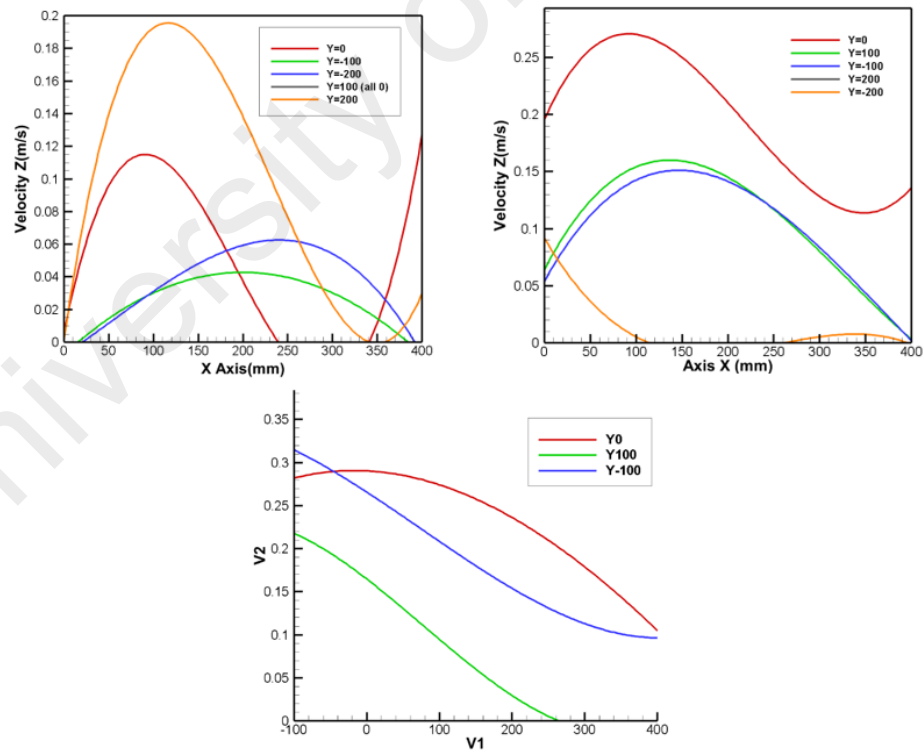


Figure 4.18 Velocity Z at Z=-100mm. Type 2 wing (Left) non-valve wing (Right) and type 3 wing (Below)

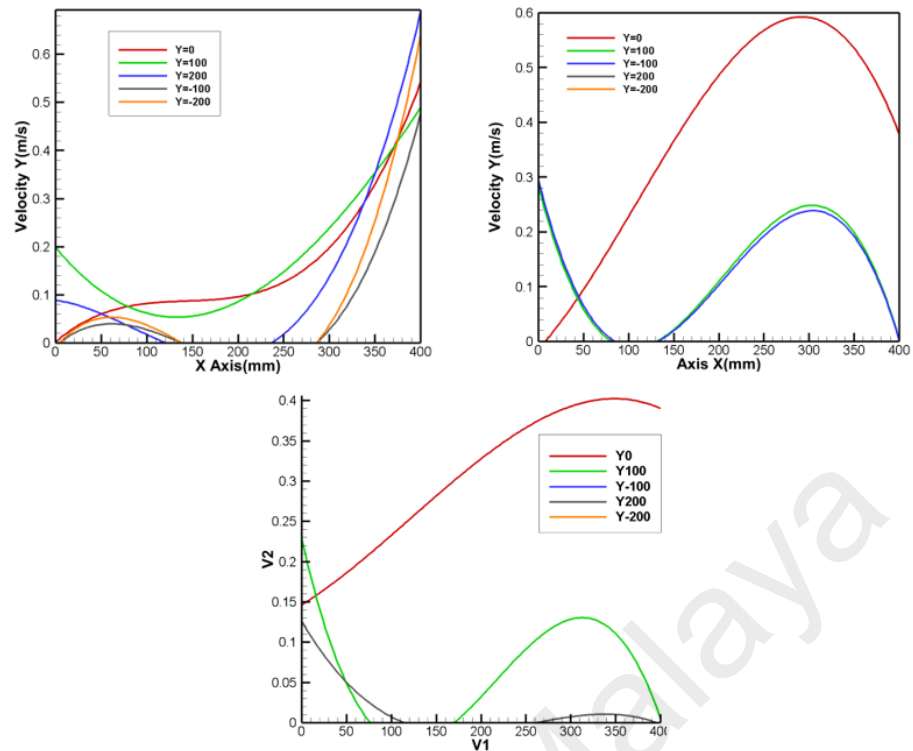


Figure 4.19 Velocity Y at Z=-100mm. Type 2 wing (Left) non-valve wing (Right) and type 3 wing (Below)

According to the three types of wings' velocity profile, it can be observed that type 3 wing has the smallest z-direction velocity at plane 1 which means the air resistance on the upper surface of the wing is the smallest among three wings. The y-direction velocity of type 3 at plane 2 is larger than no valve wing. The wind is concentrated on the central axis of the drone at plane 3 and the velocity is close to no valve wing which proves that the one-way valve has little effect on the downstroke and improved a lot on the upstroke.

The detailed description of the velocity of wings is shown in table 4.38.

As we can see, the type 3 wing has the best performance for this test and it practically reduced drag force that meets the initial expectations. The type 2 wing does not have a good result for lift and drag because of the different valve direction.

Table 4.42 Velocity description at three plane for three types of wings

Wing type	Z=100mm		Z=0	Z=-100	
	Z Direction	Y Direction	Y Direction	Z Direction	Y Direction
No valve	Fine	Fine	Poor	Fine	Good
Type 2	Poor	Fine	Good	Poor	Fine
Type 3	Fine	Poor	Good	Good	Fine

University of Malaya

CHAPTER 5: CONCLUSIONS

The goal of this research is to design and develop a wing with one way valve for flapping drone. The first part of this research used CFD simulation to verify the feasibility and principle of the one way valve. The CFD simulation included four different angle of valve (3° , 15° , 30° , 45°), two cases of inlet (two inlets and three inlets based on actual flight of flapping drone) and different number of valves (single valve and two valves). The second part of this research was to make a real prototype with one way valve on the wing to test the flight performance. There were totally four types of wings were tested. The dimension of wing was 280 mm length and 90 mm width with one row or few rows of valves. In the flight performance test, the battery life, maximum altitude, and flight stability was tested. Finally, those wings that had good performance of flight was measured the velocity of airflow generated by flapping. The results of this research can be concluded as follow:

- The one way valves perform the most effectively when the angle of the opening in the range between 30° to 45° , according to CFD simulations.
- The performance of the one way valve increases with the number of rows without affecting the structural performance of the wing which means there is an upper limit on the number of valves.
- The one way valve can increase the flight capability of flapping drone according to the actual experiment results from chapter 4.2.2.
- The direction of valves has a great influence on the flight according to the results from chapter 4.2.3.

5.1 Future work

Due to limited time, there are many things that can be improved in this experiment, including:

- Only one-way valve analysis was done in ANSYS and the analysis of the whole wing was not included. In the future, FSI will be used to conduct a comprehensive analysis of the wing motion to improve the experimental results.
- Due to the lack of measuring instruments, there is no method to measure the lift and drag of the experimental model during flight.
- The function of the controller is not enough as it cannot monitor the flapping frequency. Thus, it is very difficult to test the influence of different frequencies on the drag coefficient and lift coefficient. The test can be improved by replacing the controller with more advanced instruments.
- The position of the one way valve is also one of the factors that have a greater impact on the wing. It can be tested in various positions of the one way valve and compare the results respectively.
- In this experiment, only one material was selected as the loose leaf of the one-way valve. Different materials have different opening and closing angles during the flapping flight due to different stiffness and thickness. It can also be used for comparative tests by selecting variety of materials.

REFERENCES

- AEROVIRONMENT. (2011, 2 17). *AEROVIRONMENT DEVELOPS WORLD'S FIRST FULLY OPERATIONAL LIFE-SIZE HUMMINGBIRD-LIKE UNMANNED AIRCRAFT FOR DARPA*. Retrieved from AEROVIRONMENT: https://www.avinc.com/resources/press-releases/view/aerovirement_develops_worlds_first_fully_operational_life-size_hummingbird
- Antonia B Kesel, U. W. (1998, July). Biomechanical aspects of the insect wing: an analysis using the finite element method. *Computers in Biology and Medicine*, pp. 423-437.
- C. De Wagter, S. T. (2014). Autonomous flight of a 20-gram Flapping Wing MAV with a 4-gram onboard stereo vision system. *2014 IEEE International Conference on Robotics and Automation (ICRA)* (pp. 4982-4987). Hong Kong, China: IEEE.
- Chen L, Y. W. (2015). Experimental Validation on Lift Increment of a Flapping Rotary Wing with Boring-hole Design. *Procedia Engineering*, 1543-1547.
- CURBELL PLASTIC. (2020). *Plastic Properties Table*. Retrieved from CURBELL PLASTIC: <https://www.curbellplastics.com/Research-Solutions/Plastic-Properties>
- DELFLY. (2018). *DelFly Nimble*. Retrieved from DELFLY: <http://www.delfly.nl/>
- DELFLY. (2020). *DELFLY*. Retrieved from History: <http://www.delfly.nl/>
- Dornheim, M. (1998). Tiny drones may be soldier's new tool. *Aviation Week & Space Technology*, 42-43.

- Gao G, S. B. (2010). Study of opening holes on the wing of flapping-wing MAV and its effect on Study of opening holes. *Journal of Fluid Mechanics*, 70-73.
- Grafix. (2020). *Mylar® polyester film and sheet properties*. Retrieved from Grafix Plastics: https://www.grafixplastics.com/grafix-plastics/plastic-film-plastic-sheet-faq/mylar_what/mylar_prop/
- Hoon Cheol Park, S. Y. (2004). Design and demonstration of flapping wing device powered by LIPCA. *Proceedings of SPIE - The International Society for Optical Engineering* (pp. 212-216). San Diego, CA, United States: Society of Photo-optical Instrumentation Engineers.
- Hsu C K, E. J. (2010). Development of flapping wing micro air vehicles - Design, CFD, experiment and actual flight. *Proceedings of the 48th AIAA Aerospace Sciences Meeting Including the New Horizons Forum and Aerospace Exposition*. Orlando, USA: AIAA.
- J K Shang, S. A. (2009, August 27). Artificial insect wings of diverse morphology for flapping-wing micro air vehicles. *Bioinspiration & Biomimetics*.
- J. M. Mcmichael, C. M. (1997). *Micro Air Vehicles - Toward a New Dimension in Flight*. Arlington VA: Defense Advanced Research Projects Agency.
- Janson, S. (1995). Spacecraft as an Assembly of ASIMS. In H. Helvajian, *Microengineering Technology for Space Systems* (pp. 181-258). Los Angeles, CA: The Aerospace corporation.
- Jiaqing, C. (2014). *ANSYS FLUENT technology foundation and engineering application*. Beijing: China Petrochemical Press CO.LTD.

- Karasek M, H. A. (2014). Pitch and roll control mechanism for a hovering flapping wing MAV. *International Journal of Micro Air Vehicles*, 253-264.
- Lentink D, J. S. (2009). The scalable design of flapping micro-air vehicles inspired by insect flight. In Z. J. Floreano D, *Flying Insects and Robots* (pp. 185-205). Heidelberg, Germany: Springer-Verlag Berlin.
- Long Chen, Y. Z. (2017). Study on lift enhancement of a flapping rotary wing by a bore-hole design. *Proceedings of the Institution of Mechanical Engineers Part G Journal of Aerospace Engineering* , 1315-1333.
- Lu, Z. (2018). Bioinspired Low-Noise Wing Design for a Two-Winged Flapping-Wing Micro Air Vehicle. *AIAA JOURNAL*.
- Mackenzie, D. (2012). A flapping of wings. *Science*, 1430-1433.
- Madangopal R, K. Z. (2005). Biologically inspired design of small flapping wing air vehicles using four-bar mechanisms and quasi-steady aerodynamics. *Journal of Mechanical Design*, 809-817.
- Matěj Karásek, Y. N. (2013). Pitch Moment Generation and Measurement in a Robotic Hummingbird. *International Journal of Micro Air Vehicles*, 209-309.
- Matthew Keennon, J. G. (2014, March 11). *Development of Two MAVs and Vision of the Future of MAV Design*. Dayton, Ohio: AIAA International Air and Space Symposium and Exposition: The Next 100 Years.
- Matthew Keennon, K. K. (2012). Development of the Nano Hummingbird: A Tailless Flapping Wing Micro Air Vehicle. *50th AIAA Aerospace Sciences Meeting*

Including the New Horizons Forum and Aerospace Exposition. Nashville, Tennessee: American Institute of Aeronautics and Astronautics, Inc.

Mehdi Grommem, N. C. (2014). On the shape optimization of flapping wings and their performance analysis. *Aerospace Science and Technology*, 274-292.

Mueller D, G. J. (2009). Incorporation of passive wing folding in flapping wing miniature air vehicles. *Proceedings of ASME Mechanism and Robotics Conference*. San Diego, USA: ASME.

Nguyen Q V, C. W. (2015). An insect-inspired flapping wing micro air vehicle with double wing clap-fling effects and capability of sustained hovering. *Proceedings of the International Society for Optical Engineering*, 94290U.

Nina Gaissert, R. M. (2014). Inventing a micro aerial vehicle inspired by the mechanics of dragonfly flight. *Towards Autonomous Robotic Systems* (pp. 90-100). Springer Berlin Heidelberg: TAROS 2013.

Ning, S. (2015). *Research on Structure Design and Aerodynamic Performance of Flapping Wing Micro Air Vehicle*. He fei,China: Hefei University of Technology.

Park J H, Y. K. (2008). Designing a biomimetic orthonthopter capable of sustained and control flight. *Journal of Bionic Engineering*, 39-7.

Peng Bai, E. C. (2007, May 09). A new bionic MAV's flapping motion based on fruit fly hovering at low Reynolds number. *Acta Mechanica Sinica*, pp. 485-493.

Pornsirirak T N, T. Y. (2001). Titanium-alloy MEMS wing technology for a micro aerial vehicle application. *Sensors and Actuators A: Physical*, 95-103.

- Qi Wang, J. G. (2013). Optimal hovering kinematics with respect to various flapping-wing shapes. *IMAV 2013*, (pp. 17-20). Toulouse, France.
- Quoc V Nguyen, W. L. (2017). Experimental investigation of wing flexibility on force generation of a hovering flapping wing micro air vehicle with double wing clap-and-fling effects. *International Journal of Micro Air Vehicles*, 187–197.
- Quoc-Viet Nguyen, W. L. (2016). Hybrid Design and Performance Tests of a Hovering Insect-inspired Flapping-wing Micro Aerial Vehicle. *Journal of Bionic Engineering*, 235-248.
- RC Michelson, S. R. (1998). Update on flapping wing micro air vehicle research-ongoing work to develop a flapping wing, crawling “Entomopter”. *13th Bristol International RPV Conference*. Bristol England: 3th Bristol International RPV Conference.
- Richter C, L. H. (2011). Untethered hovering flapping flight of a 3D-printed mechanical insect. *Artificial Life*, 73-86.
- Shijun Guo, D. L. (2012). Design, Experiment and Aerodynamic Calculation of a Flapping Wing Rotor Micro Aerial Vehicle. *52nd AIAA/ASME/ASCE/AHS/ASC Structures, Structural Dynamics and Materials Conference* (pp. 4-7). Denver, Colorado: AIAA.
- Takasi Misaka, S. O. (2006). *Application of Local Correlation-Based Transition Model to Flows Around Wings*. Reno, Nevada: 44th AIAA Aerospace Sciences Meeting and Exhibit.
- ToolBox, T. E. (2010). *Lift and Drag*. Retrieved from The Engineering ToolBox: https://www.engineeringtoolbox.com/lift-drag-fluid-flow-d_1657.html

- van Breugel F, R. W. (2008). From insects to machines: A passively stable, untethered flapping-hovering micro-air vehicle. *IEEE Robotics and Automation Magazine*, 68-74.
- Wei Shyy, M. B. (1999). Flapping and flexible wings for biological and micro air vehicles. *Progress in Aerospace Sciences*, 455-505.
- Wolfgang Send, M. F. (2012). Artificial hinged-wing bird with active torsion and partially linear kinematics. *28TH INTERNATIONAL CONGRESS OF THE AERONAUTICAL SCIENCES* (pp. 1148-1157). Brisbane, Australia: ICAS 2012.
- Wood, R. J. (2007). Liftoff of a 60mg flapping-wing MAV. *Proceedings of IEEE/RSJ International Conference on Intelligent Robots and Systems* (pp. 1889-1894). San Diego, USA: IEEE.
- Xijun Ke, W. Z. (2017). Wing geometry and kinematic parameter optimization of flapping wing hovering flight for minimum energy. *Aerospace Science and Technology*, 192-203.
- Y. Nan, M. K. (2015). *An Experimental Study on Effect of Wing Geometry of Hummingbird-like Flapping Wing in the Hover*. Aachen, Germany: International Micro Air Vehicles Conference and Flight Competition.
- Yang L J, E. B. (2015). Practical flapping mechanisms for 20 cm-span micro air vehicles. *International Journal of Micro Air Vehicles*, 181-202.
- Yunus A.Çengel, A. J. (2015). *Heat and Mass Transfer*. New York: McGraw-Hill Education.

Zdunich P, B. D. (2007). Stanford S, Holeman D. Development and testing of the mentor flapping-wing micro air vehicle. *Journal of Aircraft*, 1701-1711.

Zhou Jiping, W. L. (2004). Research status and key technology of bionic flapping-wing aircraft. *Robot Technique and Application*, 12-17.

University of Malaya